Available online at www.sciencedirect.com

SCIENCE DIRECT®

International Journal of Coal Geology 60 (2004) 197–236

International Journal of COAL GEOLOGY

www.elsevier.com/locate/ijcoalgeo

The Baganuur coal deposit, Mongolia: depositional environments and paleoecology of a Lower Cretaceous coal-bearing intermontane basin in Eastern Asia

H.G. Dill[a,*], S. Altangerel[b], J. Bulgamaa[b], O. Hongor[b], S. Khishigsuren[c] Yo. Majigsuren[c], S. Myagmarsuren[c], C. Heunisch[d]

[a]*Federal Institute for Geosciences and Natural Resources, P.O. Box 510163, D-30631 Hannover, Germany*
[b]*Center of Geological Investigation, Ulaanbaatar 37, P.O. Box 318, Mongolia*
[c]*Department of Geology and Mineralogy, School of Geology, Mongolian University of Science and Technology, Ulaanbaatar 46, P.O. Box 225, Mongolia*
[d]*Geological Survey of Lower Saxony, P.O. Box 510163, D-30631 Hannover, Germany*

Received 28 April 2003; accepted 29 September 2003
Available online 13 October 2004

Abstract

The investigations involved geophysical, sedimentological, palynological, chemical and mineralogical studies, supported by field-based infrared spectrometry. The Baganuur Basin, Central Mongolia, is among the rift or pull-apart-basins, which subsided at the boundary between the Jurassic and the Lower Cretaceous in East Asia. During the Berriasian, peat accumulation began in the area under study in Central Mongolia. The palynoflora is akin to the Siberian palynological province. Based on the phytoclast assemblages and the ratios of total sulfur content to total organic content, marine transgressions into this intermontane basin may be ruled out. The coal interseam sediments were laid down prevalently under neutral to slightly alkaline conditions; only in some carbonaceous sediments, the pH of intrastratal solutions was lowered. Suboxic to anoxic conditions persisted during almost the entire Lower Cretaceous period in the Baganuur Basin. Based on the distribution of fining- and coarsening-upward sequences and the organic matter, the basin fill has been subdivided into seven depositional units (A: fluvial–swamp, B: fluvial–lacustrine, C: deltaic–fluvial, D: fluvial, E: fluvial–deltaic–lacustrine/floodplain (?), F: lacustrine–deltaic–swamp, G: swamp–fluvial). A conspicuous change in the fluvial–lacustrine regime and an increase in the sediment supply may be observed at the boundary between depositional units B and C. A strong uplift triggered the onset of an intensive delta sedimentation. Lithoclasts, heavy minerals (e.g., apatite, zircon, garnet, anatase, brookite, epidote, sphene, tourmaline) and phyllosilicates (e.g., kaolinite, smectite, mica, chlorite) attest to a mixing of detrital material. One provenance area was abundant in acidic plutonic rocks as shown by the granitic lithoclasts, the other in volcanic rocks, which produced the vitroclastic debris deposited as tephra fallout. Post-depositional alteration of the siliciclastic interseam sediments was favored by a distinctive facies association of transmissive and sealing horizons. It led to

* Corresponding author. Tel.: +49 511 643 2361; fax: +49 511 643 2304.
E-mail address: dill@bgr.de (H.G. Dill).

0166-5162/$ - see front matter © 2004 Elsevier B.V. All rights reserved.
doi:10.1016/j.coal.2003.09.008

a re-deposition of Ca, U and Sr in the siliciclastics. Post-depositional alteration of the organic material converted it into lignite to subbituminous C coal.
© 2004 Elsevier B.V. All rights reserved.

Keywords: Lignite; Cretaceous; Intermontane basin; Depositional environments; Paleoecology; Mongolia

1. Introduction

Three major geological periods are renowned for the vast accumulation of peat and formation of coal (Stach et al., 1982; Diessel, 1992; Galloway and Hobday, 1996). These are the Late Carboniferous/Late Pennsylvanian and Permian periods, the Late Jurassic through Early Cretaceous periods and the Late Paleocene and Eocene epochs, which are abundant in coal measures and which host the lion share of the world coal resources (Thomas, 2002). During earlier studies of coal deposits and coal-bearing rocks coal petrography, organic chemistry and structural geology were key elements in exploration and exploitation of this fossil energy (Stach et al., 1982; Schaefer and Püttmann, 1987; Close, 1997). In the recent past, sedimentological analyses have, in an increasing number, been used to interpret the depositional environments of coal-bearing successions (Boersma et al., 1981; Flores, 1981, 1983; Fielding, 1984, 1986; McCabe, 1984; Dill, 1987, 1989; Gentzis et al., 1990; Dill et al., 1991; Diessel, 1992; Schäfer et al., 1995; Galloway and Hobday, 1996; Markic and Sachsenhofer, 1997; Dill and Wehner, 1999; Inci, 2002). Sedimentological studies of coal measures may be useful in the prediction of coal seam geometry and quality and helpful in the exploration and exploitation of coal. Furthermore, coal-bearing strata

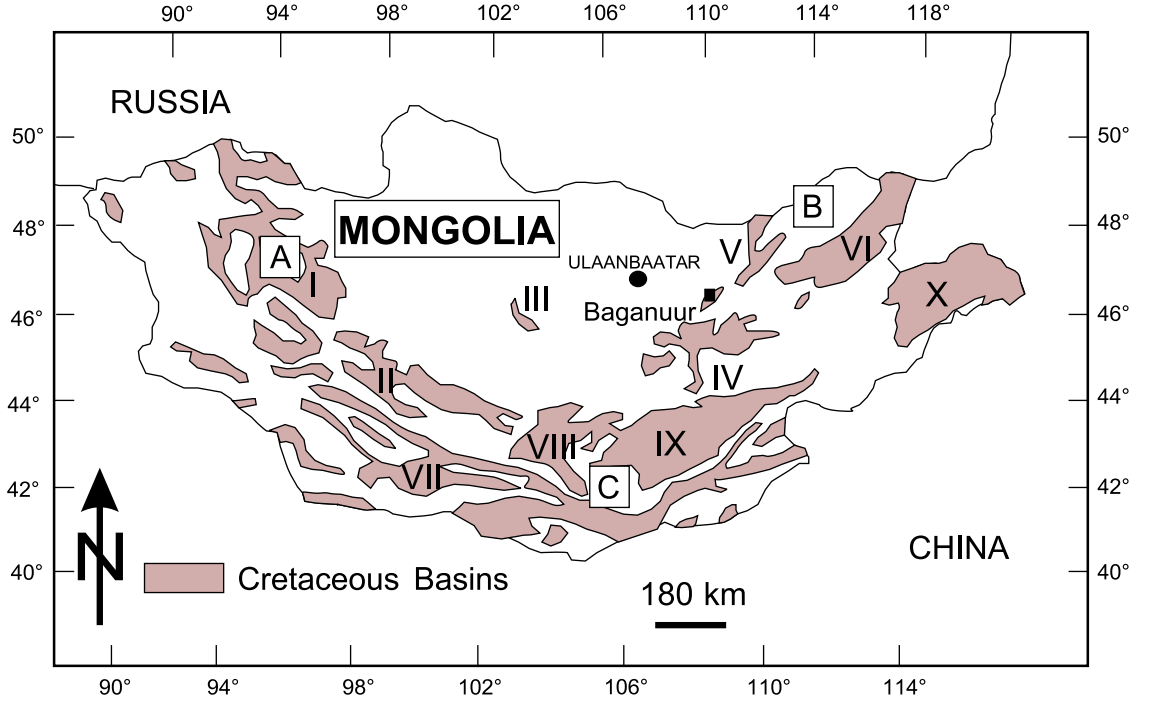

Fig. 1. Distribution of Cretaceous sedimentary basins in Mongolia (modified from Khand et al., 2000). A: Altai Province (I: Great Lakes; II: Valley of Lakes basins); B: Khangai–Khentei Province (III: Arkhangai; IV: Onon; V: Choir–Nyala; VI: Choibalsan basins); C: Gobi Province (VII: Transaltai Gobi; VIII: Umnogobi (Southern Gobi); IX: Dornogobi (Eastern Gobi); X: Tamtsag Depression basins). The study area at Baganuur is denoted by the full square.

provide an excellent target for palynological investigations. Not surprisingly, numerous studies dealing with palynostratigraphy and palynoecology were centered around major coal-bearing episodes. A few of these papers are cited herein (Pelzer et al., 1992; Malumian and Carames, 1997; Gomez et al., 2001; Tripathi, 2001).

A joint research project, involving sedimentary petrography, mineralogy and chemistry supplemented with palynological analyses, was undertaken to shed some light on the depositional environments and paleoecology of the Lower Cretaceous coal-bearing rocks in the intermontane basin of Baganuur, Mongolia (Fig. 1). The Baganuur Basin is a small depression filled with Jurassic and Cretaceous rocks between the larger Onon and Choir–Nyala Cretaceous basins (Fig. 1). The coal deposit and the large opencast mine are named after Baganuur which is the major town in this region. These Lower Cretaceous coal-bearing rocks at Baganuur warrant such an intensive scientific treatment for three reasons.

First, the location of the largest opencast mine currently in operation in Mongolia is Baganuur with reserves totaling to 600 million metric tons and an average caloric value of 3900 kcal/kg (Kampe, 1994; Jargalsaikan, 1998). Sedimentological processes exerted control on the seam geometry and the interseam lithology. A detailed investigation of the interseam sedimentary rocks may help to assess whether they might be used as a raw material, e.g, ceramic goods. To date, the interseam and overburden sedimentary rocks are being stripped off, dumped, and used for backfill.

Second, for Mongolia which is very rich in coal, this is, to our knowledge, the first study dealing with the depositional environments of the coal measures in Cretaceous rocks.

Third, the study of the very complex evolution of the carbonaceous successions in the Baganuur Basin will also help to complete the overview of the paleoclimate at the Jurassic–Cretaceous boundary in eastern Asia (Okada and Mateer, 2000). Although Cretaceous sedimentary rocks famous for dinosaur discoveries in the Gobi Desert (Benton et al., 2000) cover a large part of Mongolia, analyses of the depositional environments of these rocks are scarce and emphasis was placed mainly on stratigraphic studies (Khand et al., 2000).

2. Geological setting

Mongolia covers an area of 1,566,000 km^2, and has only a little more than 2 million inhabitants (Jargalsaikan, 1998). As part of the Central Asian Fold Belt, four east–west striking volcanic arcs have developed from the Precambrian to the Permian (Marinov, 1973; Marinov et al., 1973). Throughout the Mesozoic, tectonic reactivation triggered an intense volcanic activity and caused some basins to subside mainly in the southern part of the country (Khand et al., 2000) (Fig. 1). The Late Mesozoic basin architecture still shows the east–west trend of the ancestral volcanic arcs.

At the turn from the Jurassic to the Cretaceous, the formation of calc-alkaline plutonic and volcanic rocks, mainly granites, took place in the southern parts of Mongolia (Khand et al., 2000; Badarch et al., 2002). This Late Mesozoic igneous activity is related to the closure of the paleo-Asian and/or Mongolia–Okhotsk Oceans (Fan et al., 2003). Volcanic eruptions are a side-effect of intracontinental rifting and subsidence of basins which took up huge amounts of clastic rocks. The Jurassic to Cretaceous clastic rocks of these rift basins constitute the megasequence number four in a set of five megasequences established for Mongolia by Traynor and Sladen (1995). Megasequence four is the most prospective for fossil fuels according to the above authors. Therefore these Late Jurassic–Lower Cretaceous rocks are drilled for oil and gas and have been under exploitation for coal for decades.

Among the coal mines in this megasequence, Baganuur is the largest coal mine under operation. The coal mine is located about 110 km east of Ulaanbaatar (Fig. 1). The open pit mine in Baganuur is the major supplier for the city's power plant (Jargalsaikan, 1998). Three coal seams, as much as 38 m thick, are intercalated between clastic rocks of Cretaceous age. Conglomerates and sandstones of Jurassic to Cretaceous age underlie the coal measures. The host syncline is 3 km wide and extends about 8 km across in NNE–SSW direction (Fig. 2). The Late Mesozoic clastic rocks in the Baganuur area are overlain by Quaternary gravel and sand that attain a thickness of as much as 6 m in the study area (Fig. 3).

Cretaceous coal measures have not been studied previously in Mongolia, but attracted worldwide

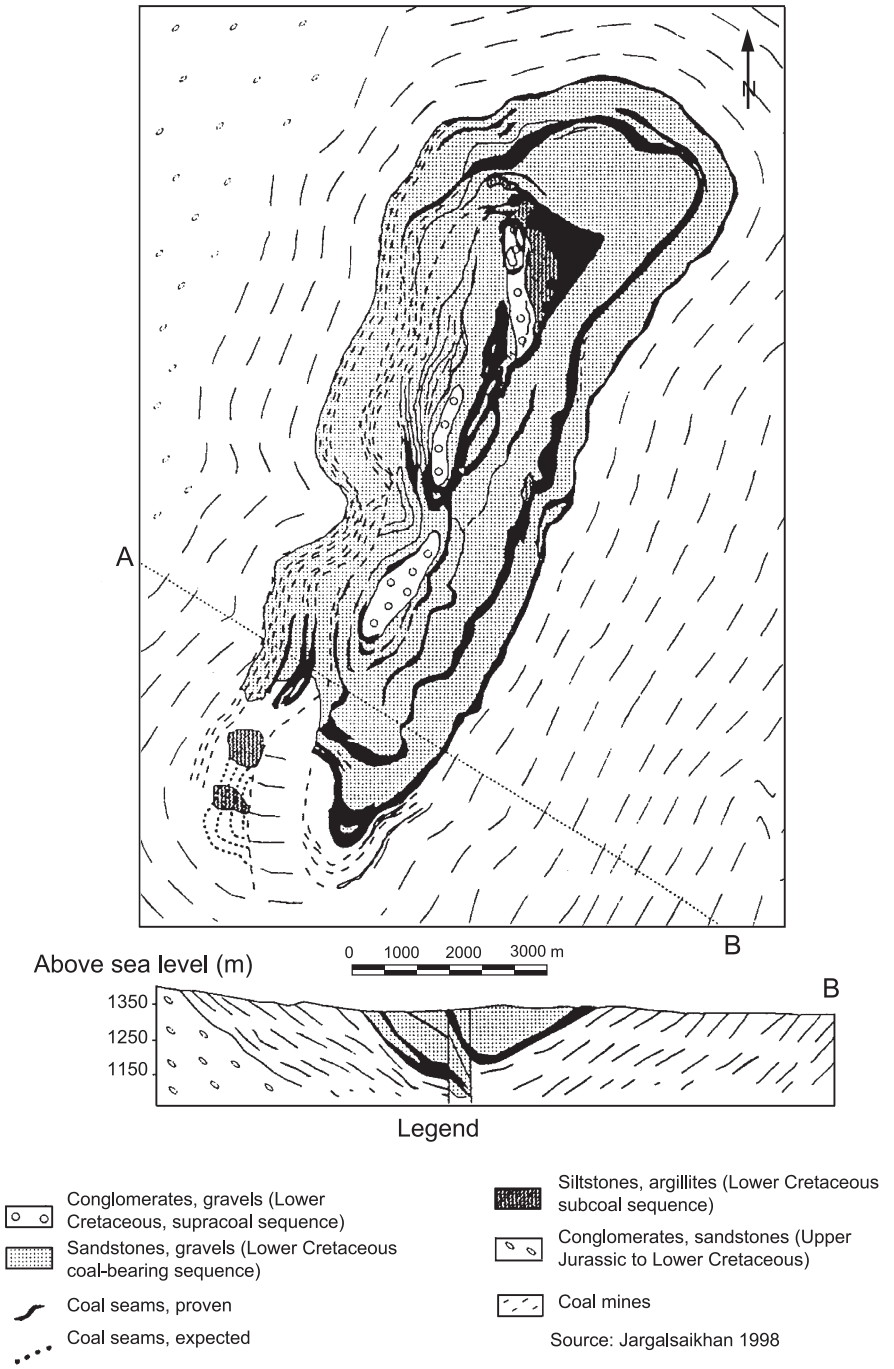

Fig. 2. Map showing the Baganuur lignite deposit and associated rocks and a cross section in the southern part of the basin (Jargalsaikan, 1998).

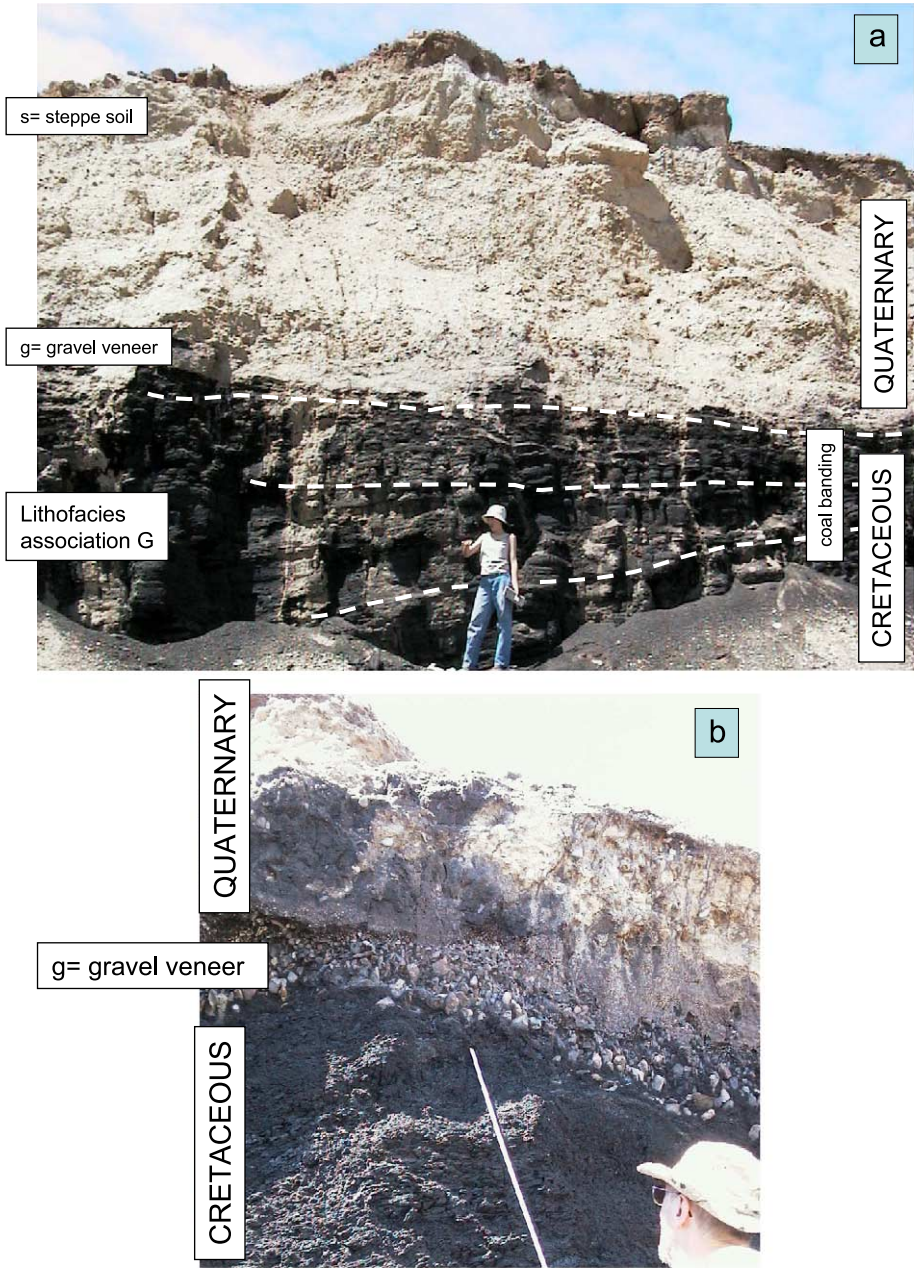

Fig. 3. Photograph showing Quaternary sediments on top of the upper coal seam of lithofacies association G. (a) Quaternary coarse-grained sediments on top of the upper coal seam are covered by a thin blanket of brown steppe soil (s) and underlain by a veneer of gravel (g) (see for close-up view figure b). Neither bedding structure nor any preferred orientation or imbrication of pebbles may be observed in the conglomerates and conglomeratic sandstones of the Quaternary overburden. In the coal seam, banding on a centimeter scale is visible (see stippled lines). In the lower part of the coal seam, the individual bedsets gently dip towards the left. Upward in the section their dip angle becomes lower. (b) Close-up view of the boundary between the Cretaceous coal seam and the Quaternary coarse-grained sediments.

attention for the coal, proper, and for the coal as a source rock for oil and gas (Clayton et al., 1991; Pelzer et al., 1992; McCabe and Parrish, 1992; Malumian and Carames, 1997; Gomez et al., 2001; Bechtel et al., 2001; Tripathi, 2001).

3. Sampling and methods

Several locations and benches in the opencast mine at Baganuur were studied and sampled in detail during the 2001 field season. A cross section across the mining benches in the western part of the open pit was studied with stratigraphic sections along ramps which cut through the zone of backfill, in the eastern part of the open pit. These sections provide a stratigraphic cross section of the entire coal-bearing Cretaceous series exposed in the Baganuur Basin.

The stratigraphic cross section was surveyed by means of a hand-held magnetometer (Kappameter) and a gamma spectrometer (Fig. 4). These geophysical methods have been discussed at length in various textbooks (Miall, 2000) and proven their applicability for correlation and interpretation of the depositional environment in many field studies. In addition to these methods, 250 samples were analyzed with a Portable Infrared Mineral Analyzer (PIMA) to collect a first-hand information in the field about the mineralogical composition of the sedimentary rocks. The results of this PIMA survey were presented in a down-hole plot similar to the geophysical logs (Fig. 5a) and compared with other mineralogical data obtained during analyses in the laboratory (Section 4.3).

IR method (infrared method), which has not yet reached routine application during sedimentological field work, is briefly described. The rocks are illuminated by an IR-light source. Certain wavelength of the light are absorbed by the rock-forming minerals as a result of sub-molecular vibrations. Bending and stretching of molecular bonds in the mineral is especially strong in minerals containing hydroxyl ($(OH)^{-}$) and carbonate ($(CO_3)^{2-}$) complexes. The spectrometer measures the reflected radiation from the surface of rocks and minerals in the short wavelength infrared (SWIR) from 1300 to 2500 nm (Fig. 5a,b). Mineral identification is based on the characteristic spectral signature of the various mineral groups such as phyllosilicates, calcareous minerals and sulfates. The IR readout of coalified matter is poor and, hence, the coal seams and lenses of organic matter may easily be identified in the set of IR spectra by their "flat" spectrum (Fig. 5a).

Laboratory-based mineralogical investigations involved examination of thin and particulate sections for the heavy mineral contents, X-ray diffraction analysis (XRD) and coal petrographic studies. Major and minor elements were analyzed using XRF. The total organic carbon content (TOC) and the total sulfur content (TS) of the samples were determined in a LECO CS 444 carbon–sulfur analyzer after removing carbonates with hot 2 N hydrochloric acid.

Nine rock samples from different lithologies in the opencast mine were studied palynologically. The composition of phytoclast assemblages (kerogen analysis) was investigated in order to constrain the age of the rocks and contribute to the interpretation of the depositional environments. The samples were prepared according to the standard palynological procedures that were elaborated in the laboratories of BGR/NLfB, Hannover (Heunisch, 1990). Prior to screening, the samples were treated with hydrochloric acid to remove calcium carbonate and hydrofluoric acid to remove silicates. After ultrasonic sieving through a 10-μm-mesh sieve, strew slides were made by mounting the particulate matter with glycerin jelly on an object slide. Some samples were in need of oxidation of the organic matter. Therefore the dissolved samples were split into two parts. Split 1 was treated with nitric acid (HNO_3). For the kerogen analysis the original, untreated sample (split 2) was selected, whereas for counting the palynomorphs the oxidized samples were used as well.

4. Results

4.1. Palynostratigraphy

All samples contain palynomorphs in sufficient quantities but in different stages of preservation (Table 1). The taxa identified in the samples point to a Lower Cretaceous age (Berriasian–Barremian)—see for palynostratigraphical comparison, e.g., Herngreen and Chlonova (1981), Zhi-chen et al. (1987) and Khand et al. (2000). The absence of the genus *Trilobosporites* and the presence of *Pilosisporites* spp. and *Aequitrir-*

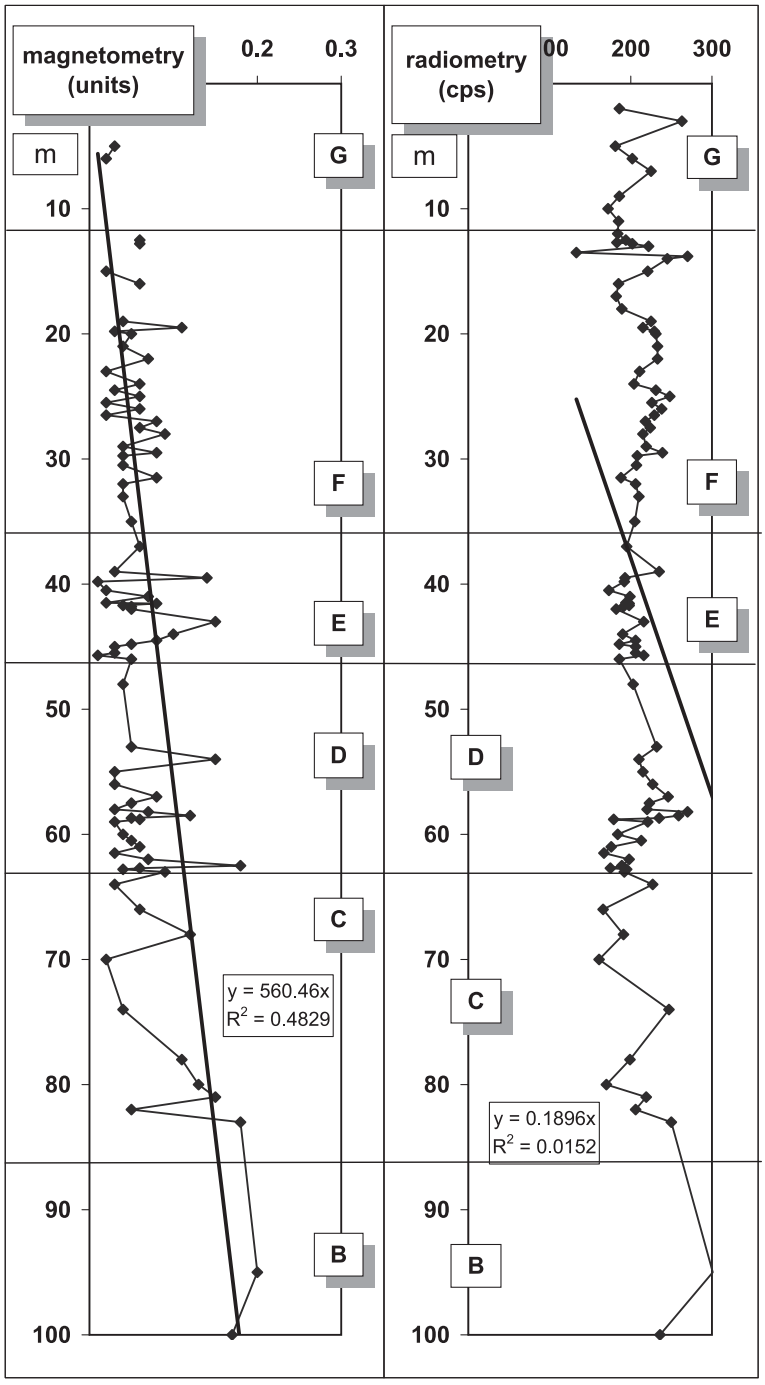

Fig. 4. Magnetic susceptibility and gamma radiation. Magnetic susceptibility (reading in units without dimension) and natural gamma radiation (total counts/ second=cps) are plotted as a function of lithology (see for more detail the individual sections of the reference cross section in Fig. 6). The trends in the geophysical logs may be deduced from y=560.46x and y=0.189x and R^2.

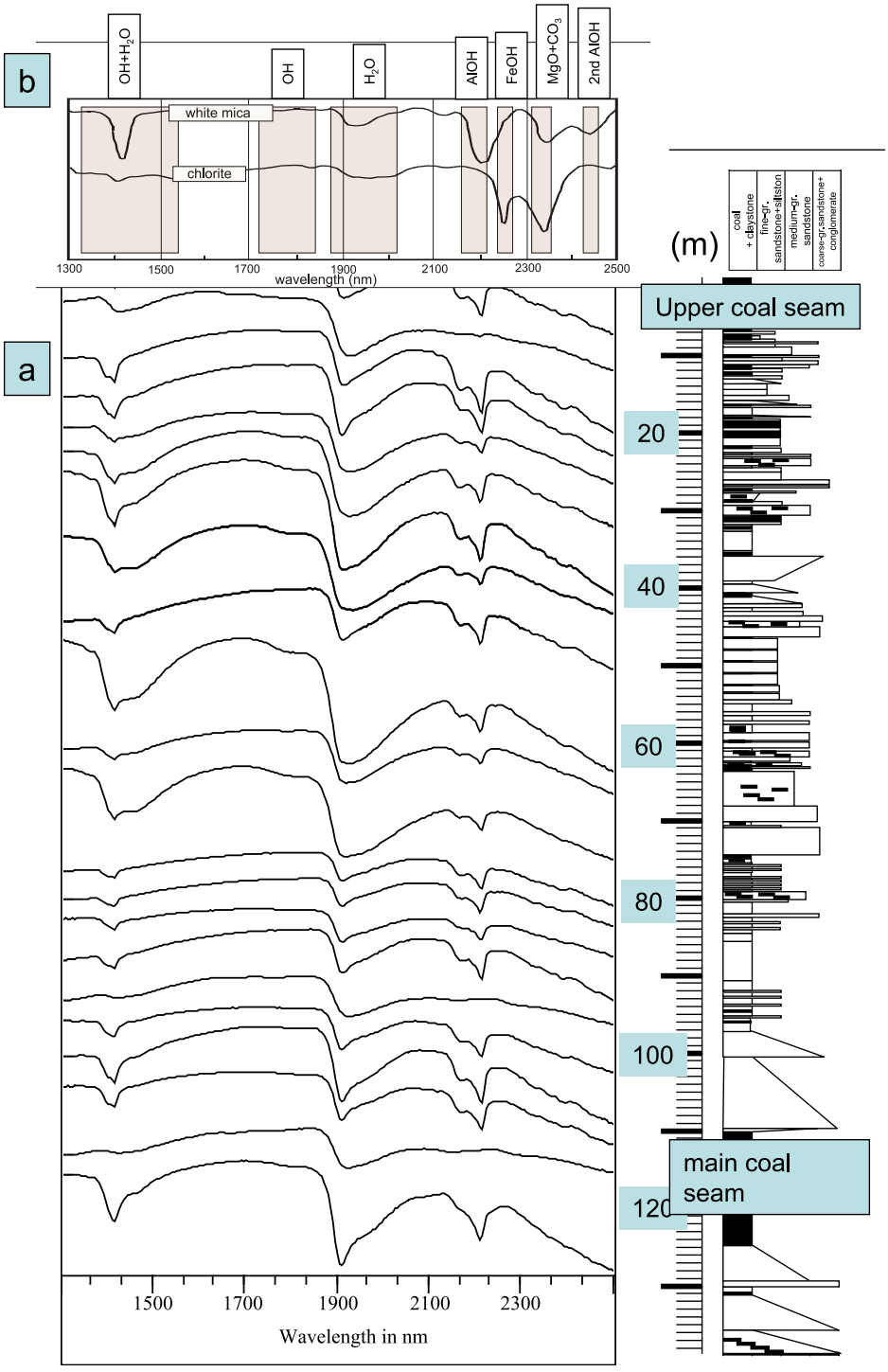
b
OH+H2O
OH
H2O
AlOH
FeOH
MgO+CO3
2nd AlOH
white mica
chlorite
1300
1500
1700
1900
2100
2300
2500
wavelength (nm)
a
1500
1700
1900
2100
2300
Wavelength in nm
(m)
coal + claystone
fine-gr. sandstone+siltston
medium-gr. sandstone
coarse-gr.sandstone+ conglomerate
Upper coal seam
20
40
60
80
100
120
main coal seam

adites spp., together with the sporadic appearance of *Corollina*/*Classopollis* spp. are typical of the Lower Cretaceous period in Mongolia. The palynoflora is akin to the Siberian palynological province, yet shows lesser similarities with the Chinese palynological province (Herngreen and Chlonova, 1981).

4.2. Lithostratigraphy, lithofacies associations and sedimentary petrography

During 2001, the Lower Cretaceous series were exposed in the Baganuur opencast mine down to a depth of about 130 m. Only the middle coal seam, called the Main Seam, and the Upper Seam were accessible out of three seams. The lowermost seam was penetrated only by drill holes. During field work in 2001, the succession of sedimentary rocks was subdivided into seven lithofacies associations, each coded with capital letters from A through G in order of decreasing age (Fig. 6). The key elements to distinguish the seven lithofacies associations are (1) content of organic matter and the quantity of coal seams in the various series, (2) grain size variation throughout basin subsidence, (3) types of stratification, (4) cyclicity of bedsets in the sedimentary record (Fig. 6; Table 2).

The rock color of the lithological series changes from light gray to black. No particular attention was drawn to this rock property by a separate column in the lithologs of Fig. 6. Shades of brown, which were locally encountered in samples from the upper mining level where lithofacies association G is exposed, are due to supergene alteration as meteoric waters percolated down into Cretaceous sediments. In lithofacies association A, yellow and brown colors in some parts of the coal seam did not originate from sedimentary or diagenetic processes either. Oxidation of pyrite was sparked by the ongoing exploitation and has set on fire, in places, the lower coal seam.

The grain size variation (Fig. 6; Table 2) of the clastic rocks under study cover the entire spectrum from clay to granules as the maximum particle size—for grain size classification used in this paper see the textbook by Tucker (2001). Their cumulative grain size distribution curves mostly fall into the range of sand with tail ends to gravelly sand and muddy sand—sensu Blair and McPherson (1999) (Fig. 7). Thick coarse-grained sandy units each with a gravel veneer at the base formed in lithofacies association A and, to a lesser extent, in lithofacies associations D through F (Fig. 6). Episodical grain size changes during the Lower Cretaceous basin subsidence produced a succession of fining- (FU sequence) and coarsening-upward sequences (CU sequence). The FU sequences consist of coarse-grained sandstone and gravel at the base and claystone on top, the CU sequences of basal silt- and claystone which from bottom to top change into coarse-grained sandstones. In some of these FU sequences, considerable compositional changes also took place (Fig. 6). In some FU sequences, the content of organic matter increased at the expense of siliciclastics such as quartz and feldspar, vertical upwards in the stratigraphic column. Lithofacies associations A, B, D and G are made up exclusively of FU sequences. Some units, such as lithofacies associations A and G, have mineable coal seams in the topstratum (Figs. 8 and 9). Lithofacies associations C, E and F are of a mixed-type composition with CU and FU sequences arranged in different orders (Fig. 6). Lithofacies associations C and F have CU sequences which were followed way up by FU sequences, whereas in lithofacies association E the successions are stacked in the reverse order (Fig. 6).

Sorting of rock types was determined by visual examination, using comparison charts such as those published by Jerram (2001). The degree of sorting varies strongly within the stratigraphic column. The poor sorting value is attained in some feldspar-enriched sandstones and in the basal conglomerates. A few samples were also checked in the laboratory and their sorting values calculated according to Füchtbauer and Müller (1970) (Fig. 7). The 75th and 25th percentiles were used for calculation of the sorting values for sand-sized material. Resultant sorting values

Fig. 5. Survey graphs of Lower Cretaceous sediments, using a Portable Infrared Mineral Analyzer (PIMA). (a) Infrared spectra were measured at various depths of the reference cross section in Baganuur open pit lignite mine (see for more detail the individual lithological sections of the reference cross sections in Fig. 6). (b) Characteristic short-wave-infrared absorption features in (hull quotient) spectra of some common phyllosilicates found in Baganuur (modified from Herrmann et al., 2001) to illustrate the variation of IR-sensitive components (e.g., AlOH) through time in the Cretaceous sediments.

Table 1
Results of palynological investigation of samples from the Baganuur Mine which show pollen and spore taxa in relation to lithology and depositional environment

a

Number of rock sample	Number of palynological sample	Lithology	Depositional Environment	Biostratigraphy	Taxa	*"Deltoidospora"* spp.	*Osmundacidites* spp.	*Cicatricosisporites* spp.	*Densosporites* spp.	*Pilosisporites* spp.	*Callialasporites* spp.	ornamented spores indet	alete bisaccate pollen grains	monolete spore, indet	*Botryococcus* sp.	*Lepolepidites* spp.	*Cycadopites* spp.	*Araucariacites australis*	*Calamospora* spp.	*Stereisporites* sp.	*Dictyophyllidites* sp.	fungal spores	*Foraminisporis wonthaggiensis*	*Perinopollenites elatoides*	*Eucommiidites* spp.	*Kraeuselisporites* sp.	*Concavissimisporites* cf. *punctatus*	*Retitriletes* sp.	*Punctatisporites* spp.	*Laevigatosporites* spp.	*Granulatisporites* sp.	*Cerebropollenites* spp.	*Taurocusporites* sp.	*Baculatisporites* spp.	*Aequitriradites* sp.	*Densoisporites* sp.	*Foveosporites* sp.	*Bullasporites* sp.	*Corollina* sp.	*Microreticulatisporites* sp. indet	*"Podosporites"* sp.	*Maculatisporites* sp.	*Spheripollenites*	*Quadraeculina anellaeformis*	*Chasmatosporites*
				Categories		B	C	C1	D	C	F	C	G	A	O1	C	E	L	B	C	C	O2	C	M	E	D	C	C	B	A	C	F	C	C	D	D	C	C	N	C	X	G	C	L	G	F
SQ 10107/162	P 72139	fine-medium gr.sandstone with plant debris	transitional	Lower Cretaceous (Berriasian - Barremian)		x	x	x	x	x	x	x	x	x	x	x																														
SQ 10107/155	P 72140	silty fine-gr. sandstone with plant debris	swamp			x	x	x		x	x	x	x			x	x	x	x	x	x	x	x	x	x	x	x	x	x	x	x	x												
SQ 10107/129	P 72141	combustible shale	swamp (?)			x	x						x																																
SQ 10107/203	P 72142	tuffaceous siltstone to fine sand with plant debris	swamp			x	x	x			x		x			x												x			x		x	x	x	cf	x							
SQ 10107/53	P 72143	siltstone	fluvial			x	x	x	x				x					x											x						cf			x						
SQ 10107/67	P 72144	combustible shale	fluvial			x							x		cf			x						x				cf	x										x	x					
SQ 10107/103	P 72145	siltstone with coal streaks	fluvial			x							x		x	x		x										x												x	x				
SQ 10107/13	P 72146	siltstone	fluvial			x	x						x			x		x				x																x	x	x	x				
SQ 10107/258	P 72147	coal	swamp			x	x	x				x	x		x	x	x	x						x			x				x							x				x	x	x	cf

Table 1 (*continued*)

b

Phytoclasts P-Nr.:	72147	72146	72145	72144	72143	72142	72141	72140	72139
Palynomorphs	1	1	25	2	4	41	1	10	4
Black wood	49		25	5	31	26	3	11	28
S.O.M., black	1	2	5		31	29		23	7
S.O.M., black-brown	32	29	10	24	48	43		29	18
Brown wood	80	16	122	7	38	50	10	57	65
S.O.M., yellow-brown	35	87	1	161	47	5	181	62	50
Plant tissue	2	65	12	1	1	5	5	8	28
Animal remains						1			
Sum	200	200	200	200	200	200	200	200	200
Facies interpretation	Swamp	Fluvial	Fluvial	Fluvial	Fluvial	Swamp	Swamp (?)	Swamp	Transitional
Palynom., categories	72147	72146	72145	72144	72143	72142	72141	72140	72139
A			2						
B	20	11	4	6	7	65		32	12
C	13	3	4	3	2	7		3	8
C1						6			4
D									1
E	1		2			1		3	
F	2								2
G	51	68	76	57	78	13		43	53
L				4				4	
M	5			6	1			2	
N								2	
O1			1					1	2
O2		3		3		4		1	1
P									1
V		1							
X	8	14	11	21	12	4		9	16
Sum	100	100	100	100	100	100		100	100

are between 2.5 and 7 so that the sediments may be ranked as poorly to moderately poor sorted.

The variation in grain shape is as strong as the variation of sorting values, particularly in the central parts of the studied section (lithofacies associations D through F). Based upon visual inspection, the particles of the siliciclastics such as quartz and feldspar were categorized as angular to rounded (Fig. 6).

Various types of stratification were recognized in the Lower Cretaceous series. Large-scale horizontal bedding with bedsets measuring up to 2 m is widespread and well exposed in many of the sandstones younger than lithofacies association D (Fig. 6), whereas planar (tabular sloping beds with an angular to tangential basal contact) and trough-shaped (concave upward, channel-like bedforms in three-dimensional view) cross-stratification is common in the rocks above and below the coal seam (Fig. 8). The faint parallel bedding in the high ash coal seam of lithofacies association A is caused by the variation in coal type and a fluctuation in the delivery of quartz and feldspar into the coal seam (Fig. 10). Horizontal bedding and lamination, as used by Lundegard and Samuels (1980), are common in most of the fine-grained heterolithic sediments (Fig. 6). By definition, heterolithic sedimentary rocks consist of thin bedsets of sand- and silt-sized material. They were described by Johnson and Levell (1995) among others. Very complex structures and palaeocurrent patterns are found in heterolithic sandstones near the basis of lithofacies association C (Fig. 11).

The internal structure of these heterolithic sandstones is characterized by wave-formed ripple bedding some cm thick with discordant internal laminae. The structure is highlighted by coal streaks along the discrete laminae. The wave-formed foresets show a

tangential base that displays mud-coal drapes along their lateral extent. Flaser-bedding sensu Reineck and Singh (1980) with some coalified matter and mud forming the disconnected flasers and laminae are well developed in the basal gray successions at the boundary between lithofacies associations C and D.

The geometry of the sedimentary rocks may be subdivided into various elements, listed in Table 2. Concave-up sand bodies with and without erosional base are common on various scales. Some may attain up to 6 m in thickness. Coarse-grained lag deposits and gravel veneers were named as gravel bars. They

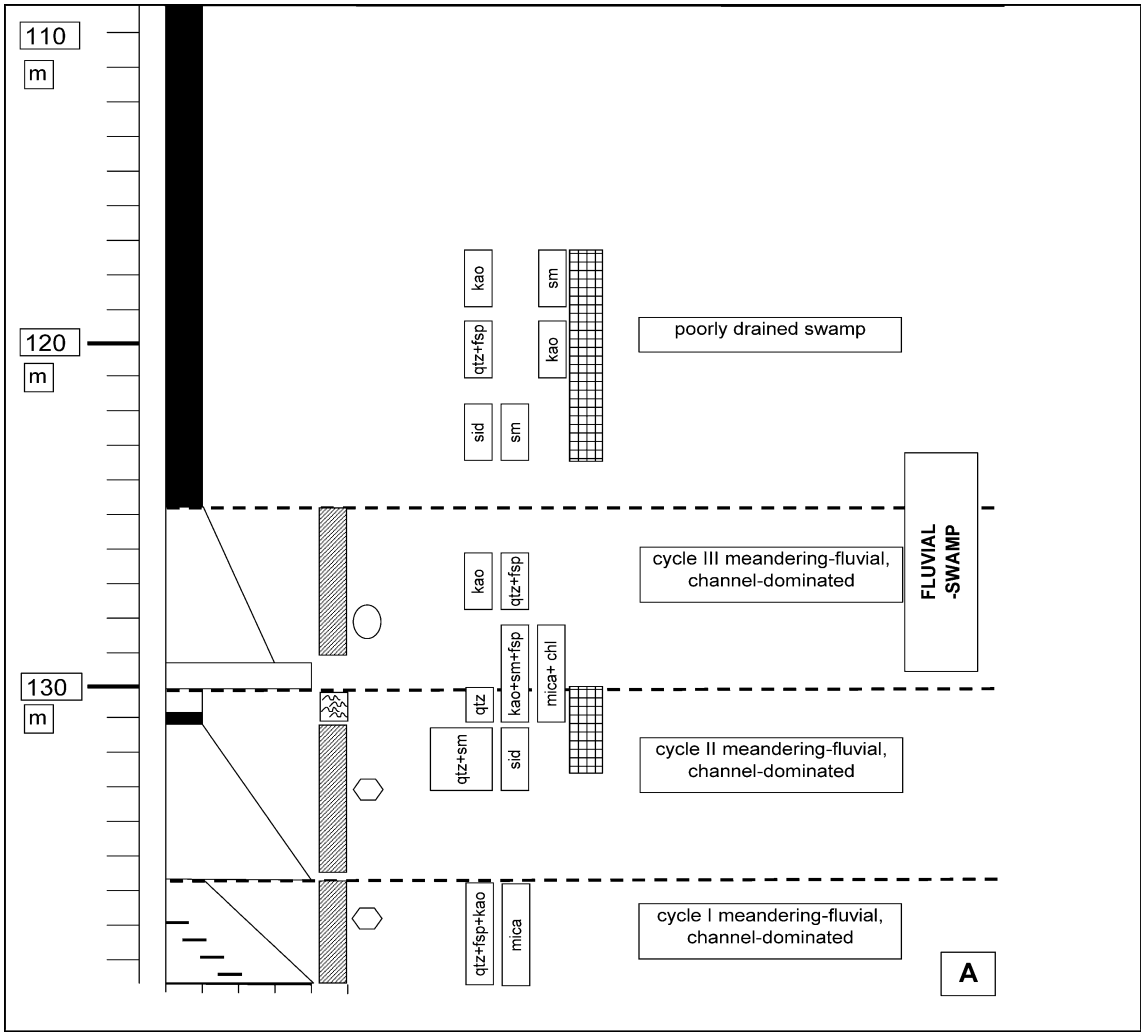

Fig. 6. Close-up view of the lithology, mineralogy and the environment of deposition of the Lower Cretaceous lithofacies associations: (A) lithofacies association A, fluvial depositional environment and swamps; (B) lithofacies association B, fluvial and lacustrine depositional environments; (C) lithofacies association C, deltaic and fluvial depositional environments; (D) lithofacies association D, fluvial depositional environment; (E) lithofacies association E, fluvial–deltaic–lacustrine/floodplain environment of deposition; (F) lithofacies association F, lacustrine–deltaic environment of deposition and swamps; (G) lithofacies association G, swamps and fluvial environment of deposition. Mineralogy: qtz=quartz, mica=white and dark mica, ca=calcite, sid=siderite, sm=smectite, fsp=alkaline feldspar, kao=kaolinite group sheet silicates, amorph=X-ray amorphous matter, chl=chlorite, pyr=pyrite, gyp=gypsum, e.g., 280°/15°=direction and dip angle of foresets in cross-stratified bedsets.

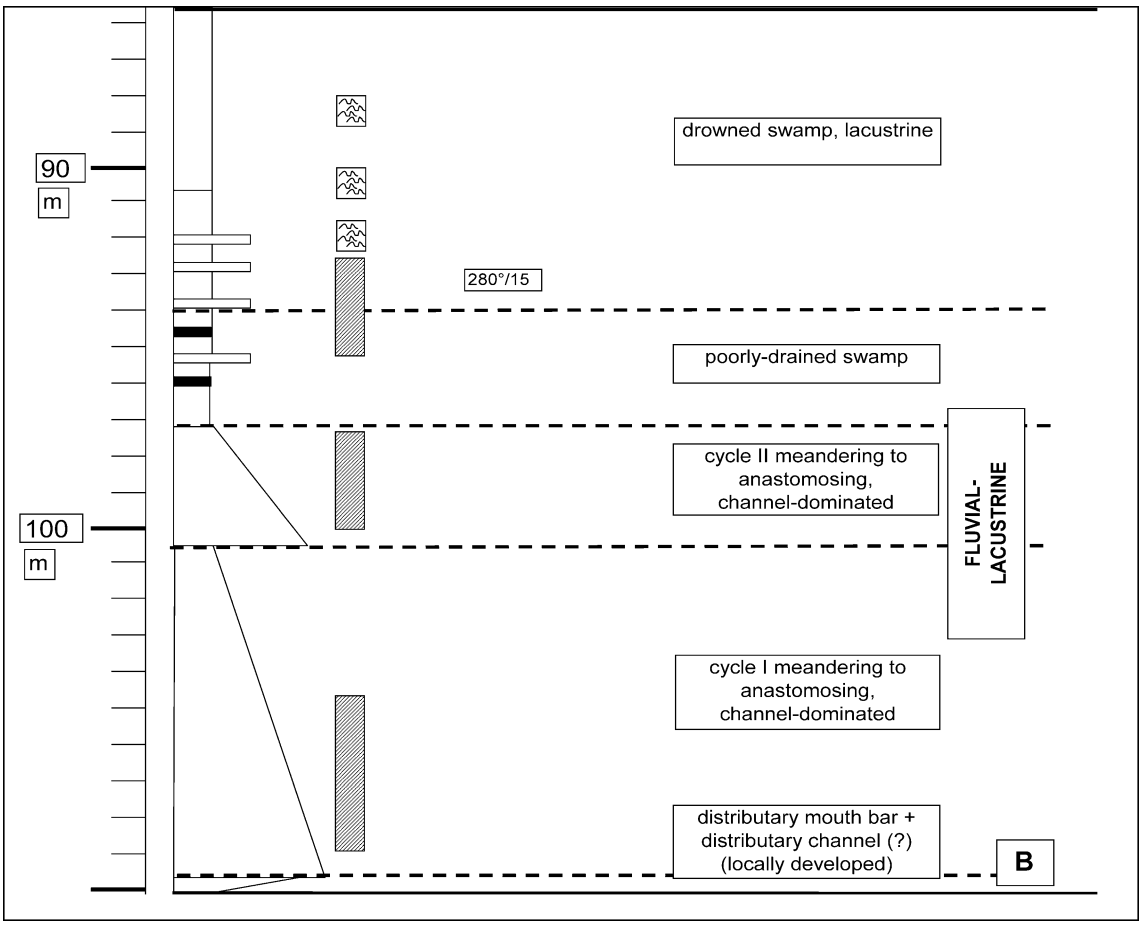

Fig. 6 (*continued*).

measure up to a few decimeters in thickness. Sheet sands have a pit-wide lateral extension and measure up to 1 m in thickness. Those beds which do not display any conspicuous stratification on the centimeter or decimeter scale were categorized as massive. The term lateral accretion macroforms was used to describe large wedge-shaped bedsets in lithofacies associations A and B. They measure several meters in thickness and show different orientations and angles of dip.

The contact between coal and interseam sediments as well as the contact between particles of organic matter and the siliciclastic rocks are important bearing in the interpretation of the depositional environment. In the succeeding paragraphs, type localities and examples within the Baganuur opencast mine are described. The examples are discussed in order of increasing scale from pit size to grain size.

Along a SE–NW cross section through the northeastern stope of Baganuur opencast mine, the spatial relationship between coal and its interseam sediments is well exposed (Fig. 8). The contacts between the coal seam and the over- and underlying sedimentary rocks are different in the various parts of the cross section. Underlain by sandstone, the coal seam shows a sharp conformable contact in the southeastern part of the cross section in Fig. 8. By contrast, in the sandstone overlying the coal seam, the cross-stratification is gently dipping towards the northeast and ends up in an erosional contact against the coal seam in the southeastern part. In the northwestern part of the cross section the sandstone beds rest conformably

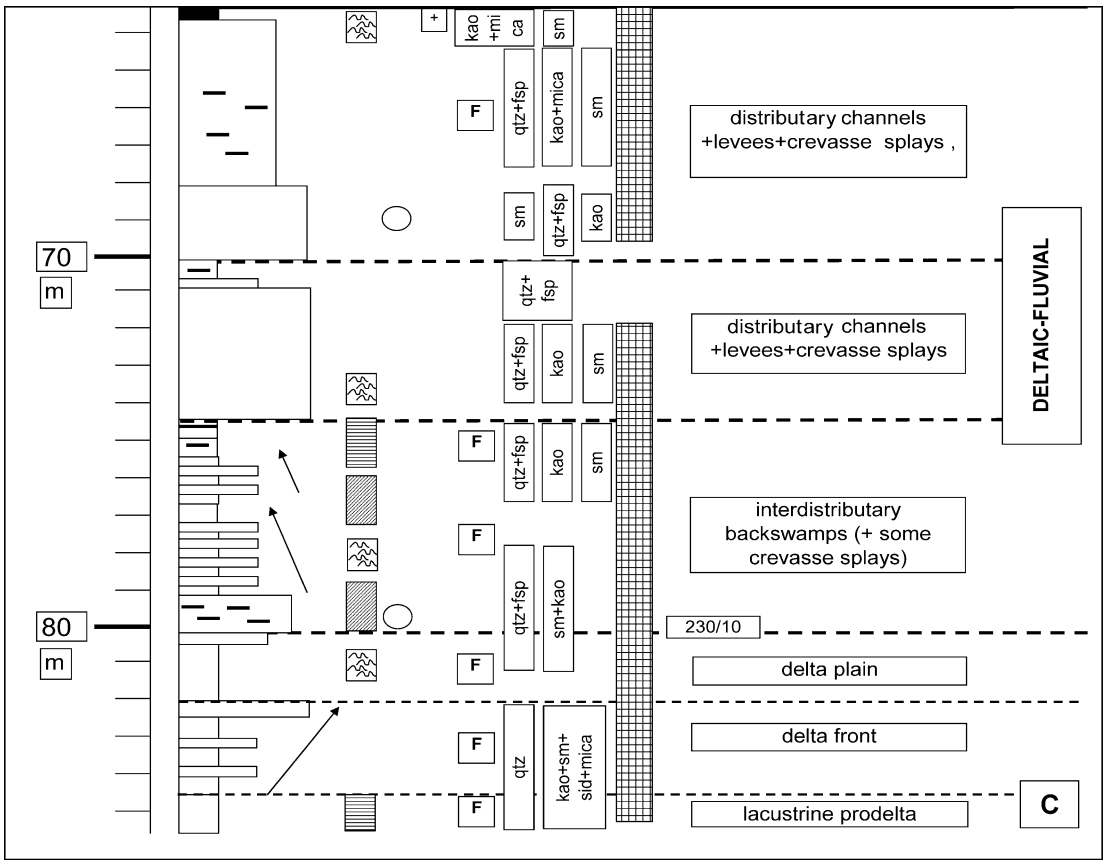

Fig. 6 (*continued*).

on the coal seam and an erosional contact exists between the coal seam and its underlying sandstone. Some bounding surfaces may be recognized in the complex bedsets of the floor rocks. They are highlighted by pencil markings in Fig. 8. The overlying sandstone truncates and splits the coal seam (Fig. 8).

In Fig. 9a, the NNE–SSW longitudinal section provides an overview of the contact between the lower coal seam and the sandstone roof sediments of lithofacies association B in the central part of the opencast mine. The bedding planes of the bedsets become steeper towards the SW resulting in an unconformity between the coal seam and the sandstone roof sediments.

In the FU sequences of lithofacies association A each sequence is composed of coarse-grained to conglomeratic arkosic sandstones at the base, which gradually convert into fine sandstone towards the top. These siliciclastics are overlain by high-ash coal seams, each showing a gradual transition into the underlying sandstone and a sharp erosional contacts towards the overlying basal conglomerates (Figs. 6 and 9b). Medium-grained sandstones of lithofacies association F with intercalated coal lenses and two thin coal seams of up to 0.2 m near the top are portrayed in Fig. 12. The coal seams have wavy roof and nearly planar floor contacts. The Upper Coal Seam gradually develops from the underlying sandstone, where at least three FU cycles may be recognized in the siliciclastics (Figs. 6 and 10). Each cycle underneath the coal seam becomes more abundant in organic matter vertically upwards, eventually leading to a layer of more or less pure organic matter of the Upper Coal Seam (Figs. 6 and 10). In the Upper Coal Seam, bands of mudstone on a centimeter scale are visible. In the lower half of the coal seam, these bands show a gentle dip. Near the top of the section their dip angle gets lower. The topmost bedding planes in the coal seam are sub-

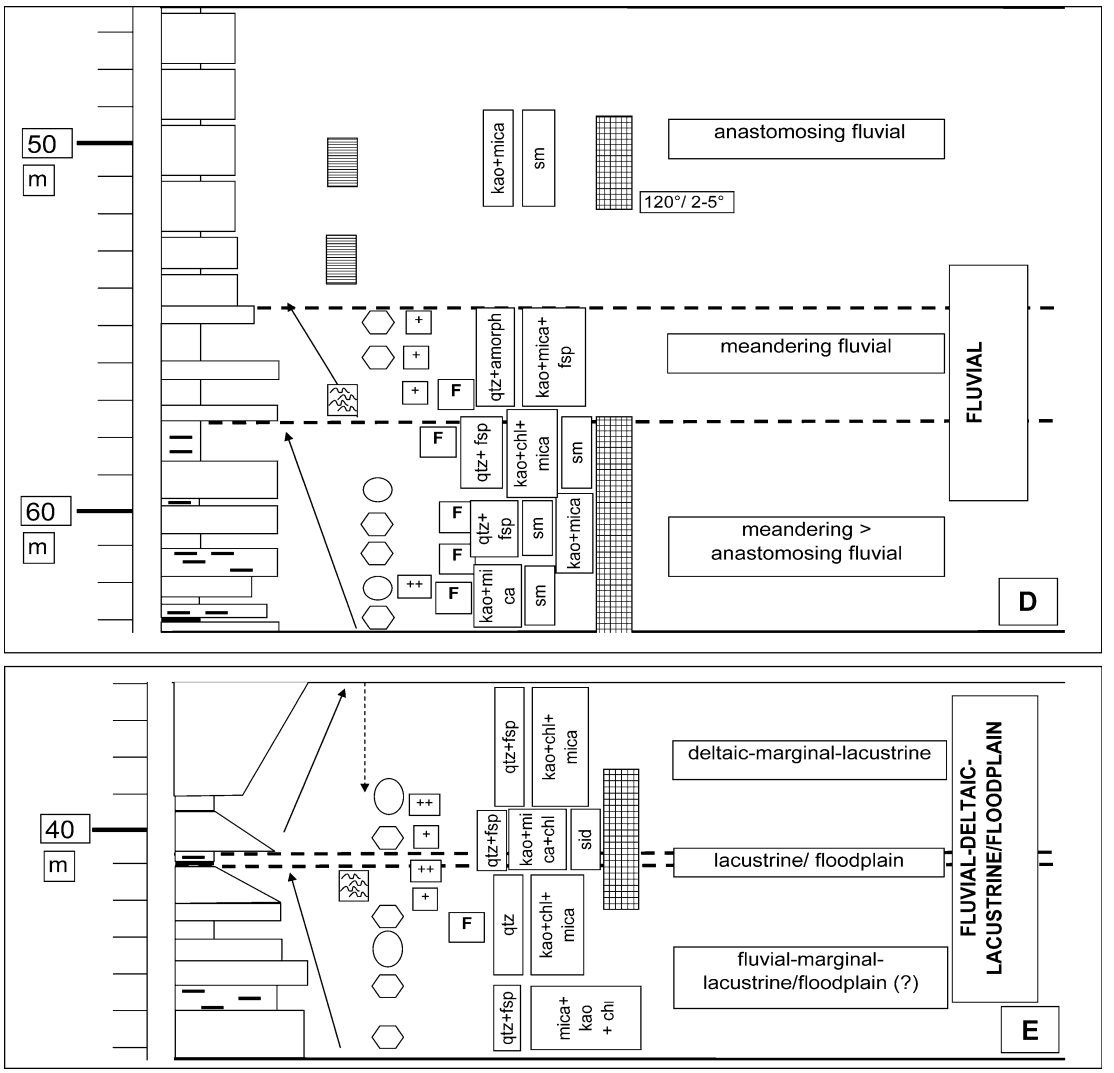

Fig. 6 (*continued*).

horizontal, giving rise to a disconformity between the Lower Cretaceous strata and the Quaternary overburden. The boundary is marked by gravel lag deposits shown in Fig. 3b.

Tree trunks in growth position have been preserved only in dark gray siltstones with fine- and medium-grained sandstones of lithofacies association C (Fig. 13). The diameter of the tree trunk measures approximately 0.2–0.3 m. Overlying these strata, broken tree trunks were found in coarser-grained sandstones of lithofacies association C, which are drift woods and aligned along the paleocurrent. Lithofacies association B is rife with fine-grained organic matter consisting of dark horizontally bedded gray mudstones and siltstones alternating with bright gray fine-grained sandstones. Some siltstones are abundant in disseminated plant debris and, consequently, be termed as Cpm-horizons (=comminuted plant material).

4.3. Mineralogical composition

Quartz and feldspar (albite-oligoclase, microcline) are the major minerals in the sandstone. Thus the majority of clastic rocks may be designated as arkosic

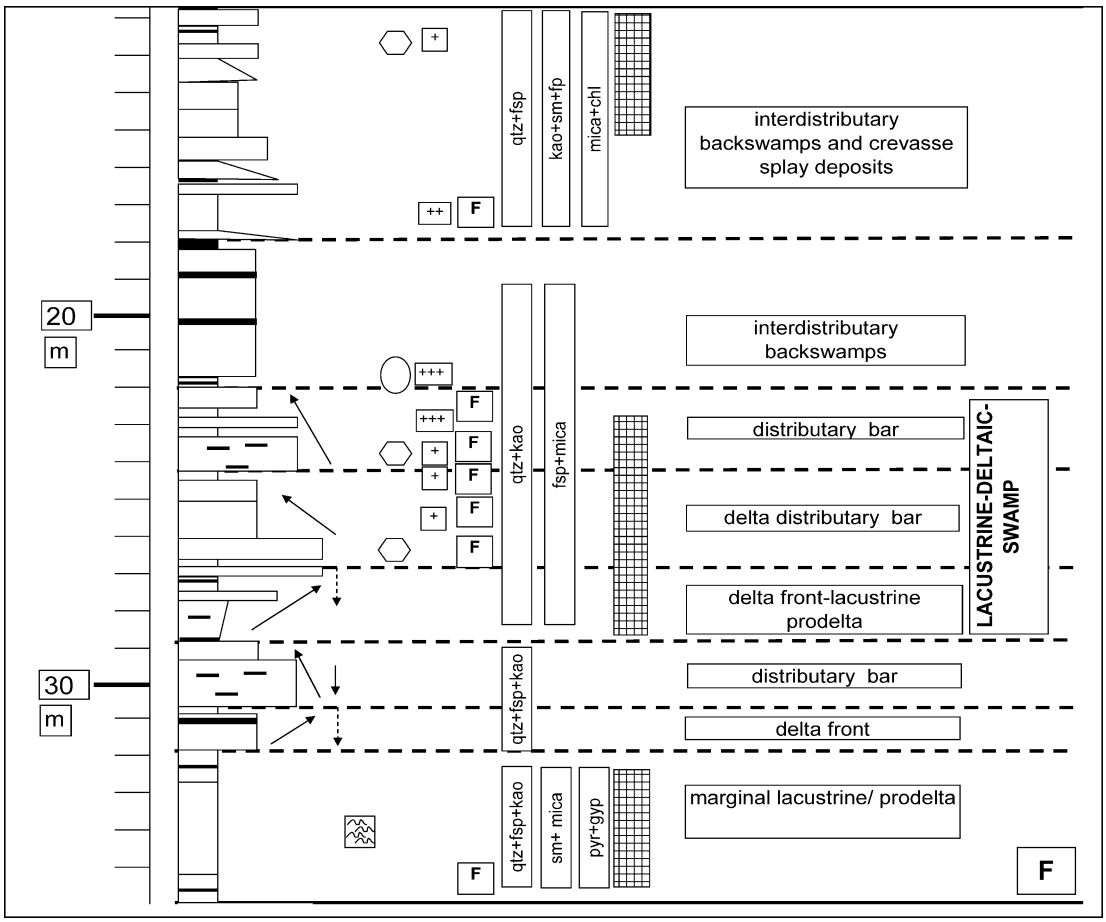

Fig. 6 (*continued*).

arenites using the classification scheme for sandstones by Pettijohn et al., (1987). Those terrigenous clastic rocks with elevated contents of lithoclasts (granitic igneous rocks, glass shards) are called lithic arkose or lithoclast-bearing feldspar arkose. In the siltstones and mudstones kaolinite-group phyllosilicates are predominant. Second most common among the sheet silicates are smectite-group phyllosilicates. Mica-group phyllosilicates (illite, muscovite and chloritized biotite) are ubiquitous and found in the arenaceous as well as argillaceous sediments in Baganuur. Siderite is the only non-silicate mineral among the rock-forming mineral. Pyrite and chalcopyrite are sparse.

To determine the distribution of minerals and fragments across the entire Lower Cretaceous, semi-quantitative XRD and IR mineral analyses were performed (Fig. 5). These analyses reveal no trend or preferred concentration of minerals through time (Figs. 5 and 6). Siderite, enriched in carbonaceous clastic rocks and coal, is an exception.

Heavy minerals may reflect the lithological composition of the provenance area and provide an idea of the chemical weathering throughout deposition of the sediments (Dill, 1995, 1998). In the study area, the assemblage of transparent heavy minerals consists of stubby crystals of apatite, elongated and stubby crystals of zircon and angular garnet. Minor components are monazite, anatase, brookite, epidote, sphene and tourmaline.

4.4. Chemical composition

The variation of the chemical composition may be deduced from the mean, maximum and minimum

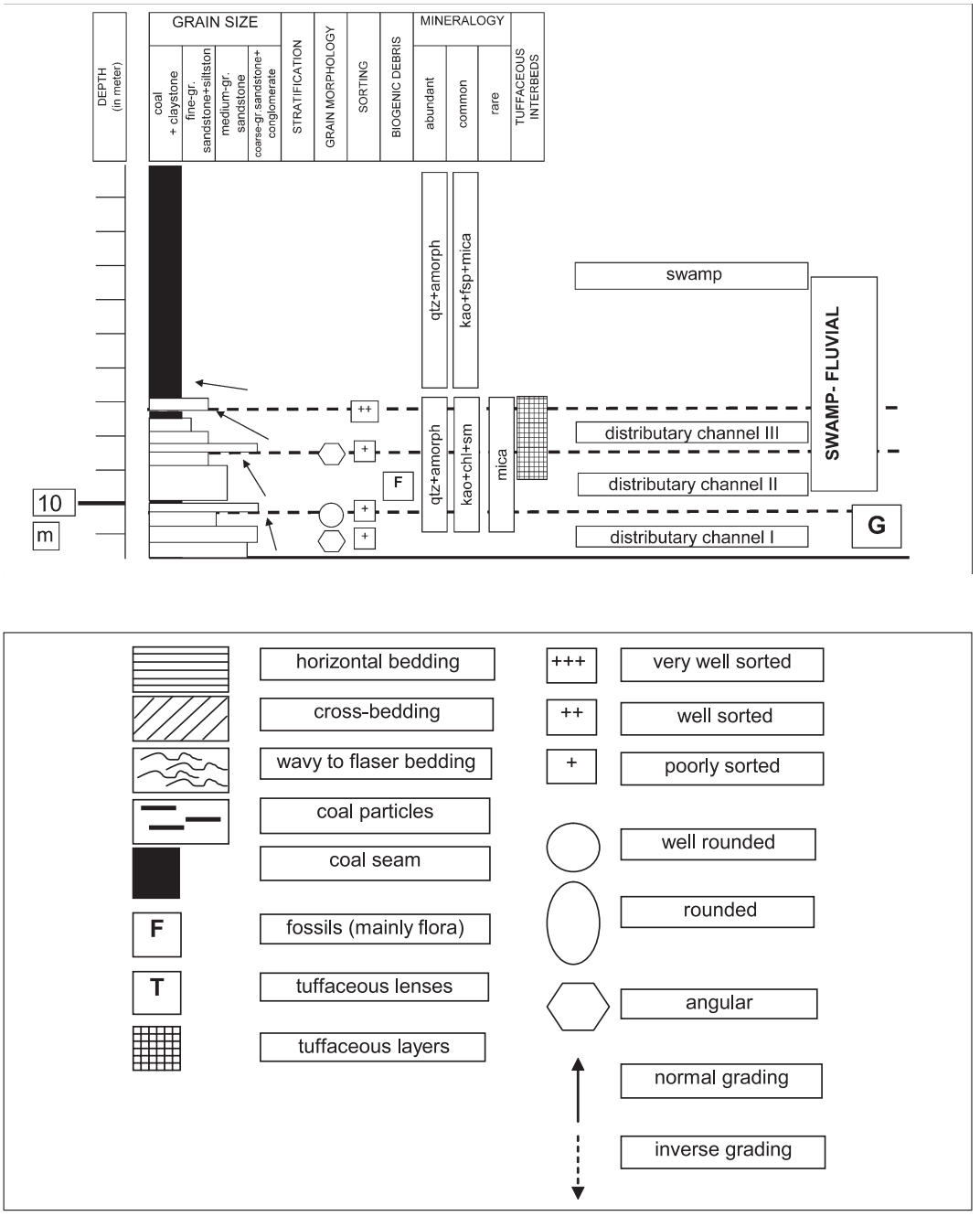

Fig. 6 (*continued*).

values listed in Table 3. Multi-element correlation was performed to put some constraints on the mineral assemblage of the Lower Cretaceous rocks and unravel the genetic relations (Table 4). To get a better view on the variation of the chemical composition of the Lower Cretaceous sedimentary rocks as a function of paleogeography and paleoecology, chemologs were designed for some relevant major and trace elements

Table 2
Lithofacies association, sedimentological data and the interpretation of the depositional environment

Lithofacies association	Lithology	Grain size	Sorting	Stratification	Geometry	Grading	Grain shape	Interpretation of the depositional environment
G	coal>>siliciclastics coal content increasing upward (bottom: coal lenses, top: coal seam)	coarse- to fine-gr. sandstone, clay, mainly medium-gr. sandstone	poorly to well sorted	horizontal, low-angle tabular cross-stratification	channels, massive layers	normal grading, FU sequences (thickening-upward) 3 cycles	angular to well rounded	swamp–fluvial
F	siliciclastics>coal, coal occurs in lenses and seams, floral remains, tuffaceous rocks	coarse-gr. to fine-gr. sandstone, clay, mainly fine to medium-gr. sandstones	poorly to very well sorted	horizontal, low-angle tabular and trough cross-stratification, flaser bedding	channels, sheet sands	normal and inverse grading, FU and CU	angular to subrounded	lacustrine–deltaic–swamp
E	siliciclastics, very little drift wood and floral remains, tuffaceous rocks	coarse-gr. to fine-gr. sandstone, clay, mainly coarse-gr. sandstone	poorly to well sorted	horizontal, low-angle tabular cross-stratification, flaser bedding	massive, sheet sands	normal and inverse grading, FU and CU	angular to subrounded	fluvial–deltaic–lacustrine/ floodplain (?)
D	siliciclastics>>coal, coal content very low, coal occurs in nests, drift wood, floral remains, tuffaceous rocks	conglomerate, coarse-gr. to fine-gr. sandstone, clay, mainly medium-gr. sandstone	poorly to well sorted	horizontal, tabular>> trough cross-stratification, little flaser bedding	channels, gravel bars, sheet sands	normal grading, FU sequences (2 cycles)	angular to well rounded	fluvial
C	siliciclastics>>coal, coal content very low, occurs in lenses and nests, drift wood, floral remains, tuffaceous rocks	conglomerate, coarse-gr. to fine-gr. sandstone, clay	not determined for the whole unit, in places, well sorted topstratum	trough cross-stratification, tabular cross stratification, flaser bedding, horizontal bedding	channels, massive	normal and inverse grading, FU (3 cycles) and CU (1 cycle)	predominantly well rounded	deltaic–fluvial
B	siliciclastics>>coal, content very low, coal occurs in lenses	conglomerate, coarse-gr. to fine-gr. sandstone, clay	poorly to moderately well sorted	trough cross-stratification, tabular cross stratification, flaser bedding	channels, gravel bars, massive layers, sheet sands, wedge-shaped lateral accretion macroforms	normal grading, FU sequences (thickening-upward) several cycles	angular to subrounded	fluvial–lacustrine
A	coal ≅ siliciclastics, coal content increasing upward (bottom: coal particles, top: coal seam), tuffaceous rocks	conglomerate, coarse-gr. to fine-gr. sandstone, clay	poorly to moderately well sorted	trough cross-stratification, tabular cross stratification, flaser bedding	channels, gravel bars, massive layers, wedge-shaped lateral accretion macroforms	normal grading, FU sequences (thickening-upward) 3 cycles	angular to subrounded	fluvial–swamp

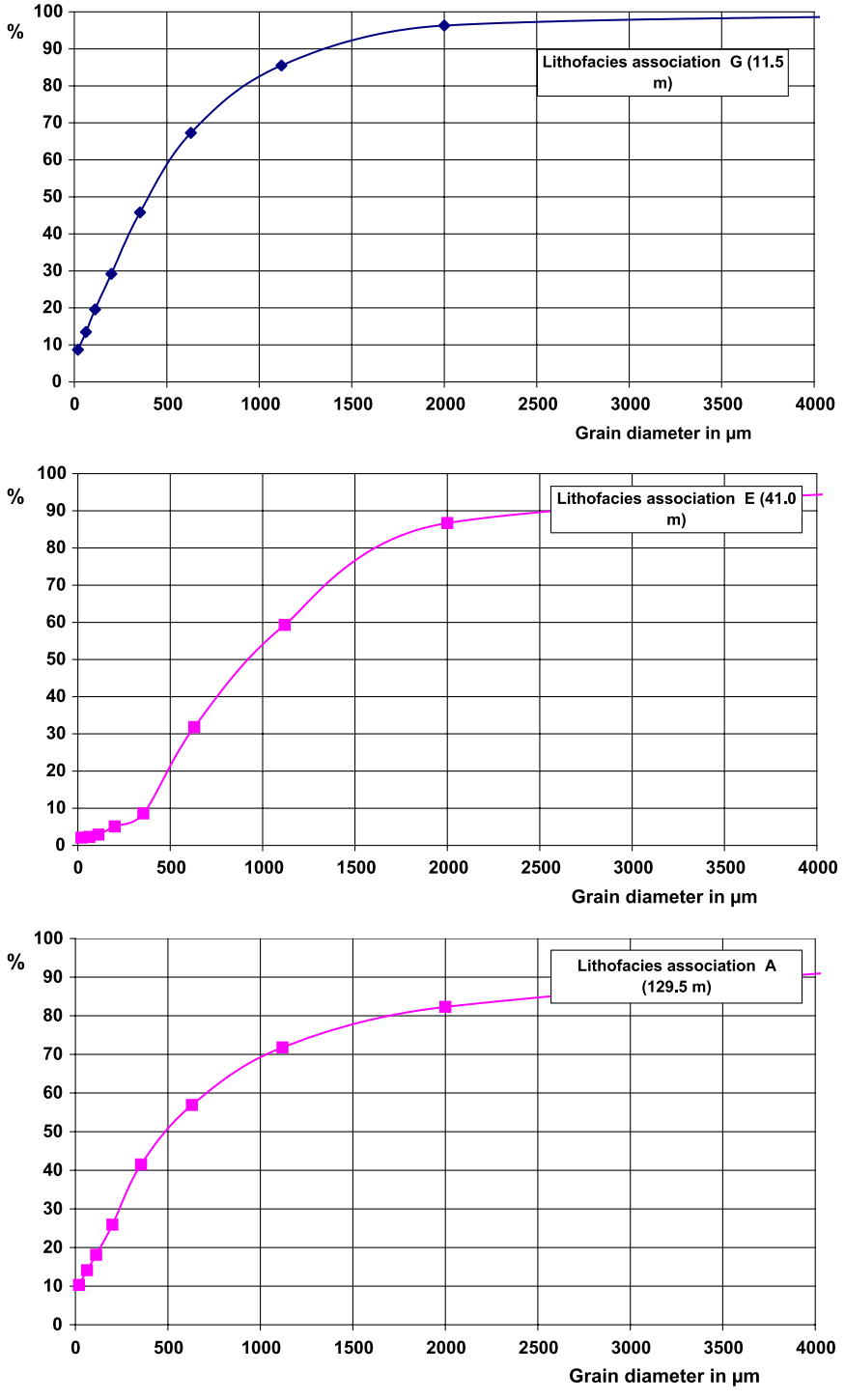

Fig. 7. Cumulative grain size distribution of interseam sediments in the Baganuur open pit mine.

Fig. 8. SE–NW cross section along the northeastern stope of the Baganuur open pit. The photograph shows the contacts between the lower coal seam and roof and floor rocks as well as seam split (dotted line). Bedding planes and bounding surfaces within the interseam sediments are highlighted by heavy lines.

(Fig. 14). The chemical composition of the Lower Cretaceous rocks was subjected to considerable changes with basin subsidence. This is not surprising in view of the conspicuous grain size variation shown by the FU and CU successions in the study area (Fig. 6). Decreasing- or increasing-upward chemical compositions may be recognized for some major and minor elements in the chemolog. These trends common to more than one element are the basis for categorization into what may be called paragenetic chemical associations.

The contents of Ti, Al and Fe increase vertically upward in the stratigraphic column. The major elements reach a relative maximum of mean values in lithofacies association C and attain significantly lower mean values in lithofacies association G. The mean values calculated for lithofacies associations A and G are almost identical (Fig. 14). This holds true also for the distribution of the trace elements Th and Zr. The distribution of silica yields a similar curve, but it is less pronounced than those of Ti, Al and Fe. Despite its deviation from the common trend, it is grouped together with Ti, Al, Fe, Th and Zr for generic reasons.

The trace elements U and Sr display a polymodal distribution with three maxima (Fig. 14). Calcium is the only major element that shows a good match to the distribution curves of U and Sr. The distribution curves of Co and Zn go together, whereas the distribution curves of Cu and the aforementioned base metals are a bad match.

In the matrix diagram of Table 4b, only those element couples which have correlation coefficients of $r > 0.75$ are recorded. The first column in the matrix denotes the mineral group which hosts the elements listed in the succeeding columns.

The total organic carbon content/total sulfur content ratio (TOC/TS) has proven to be a very efficient

Fig. 9. Photographs showing the contacts between the coal seams and their interseam sedimentary rocks. FU sequences are marked by the wedge-shaped symbols. The rose diagrams illustrate the paleocurrent trends in the siliciclastics. For scale see power line post (top left) measuring approximately 4 m in height. (a) A photograph showing a NE–SW longitudinal section of the sandstone roof rocks of lithofacies association B in the central part of the open pit and the lower coal seam of lithofacies association A. The bedsets become steeper towards the SW creating an unconformity between the coal seam and the sandstone roof rocks. Lithofacies association B is composed of FU cycles each with fine-grained dark siliciclastics on top and white coarser-grained sediments at the base. The top of the coal seam is highlighted with a bold-faced stippled line, the upper boundary surface of the individual FU cycles is marked with full lines. (b) A haulage ramp through lithofacies A in the eastern part of the open pit provides an overview of the FU sequences which belong to cycles I and II of lithofacies association A. Each sequence is composed of coarse-grained to conglomeratic arkosic arenites at the base that gradually convert into fine-grained sand vertically upward. The siliciclastics are overlain by high ash lignite seams.

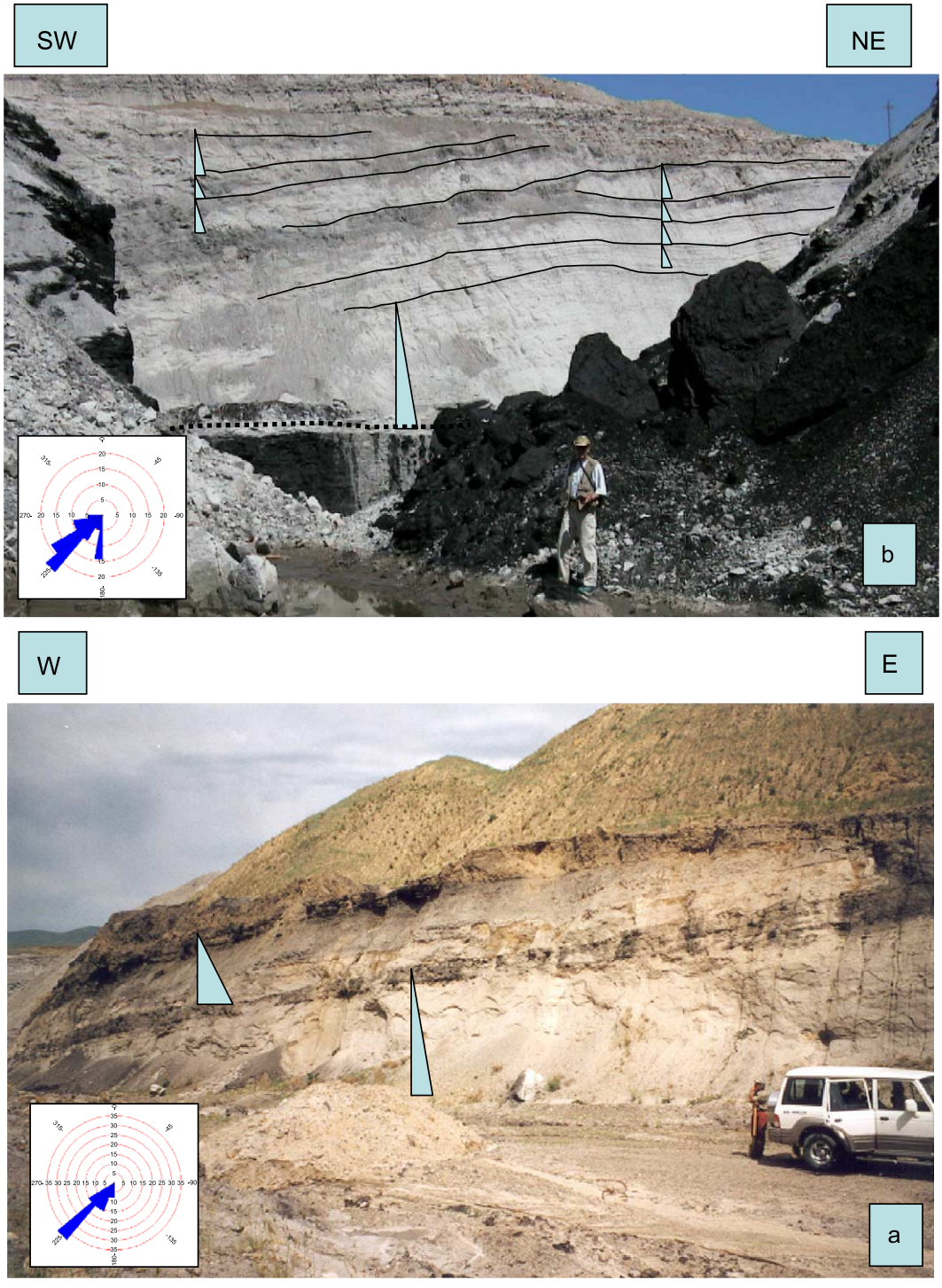
SW
NE
b
W
E
a

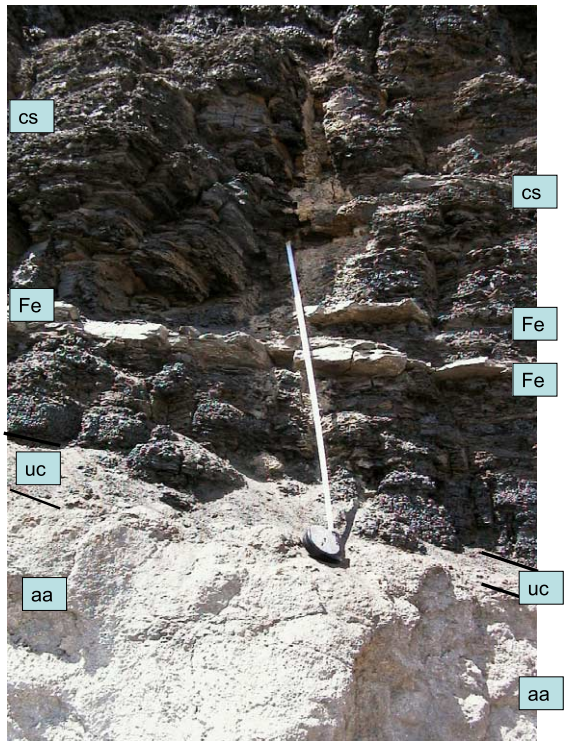

Fig. 10. Photograph showing the contact between the Upper Coal Seam (cs) and its floor rocks (aa). The contact between both strata is transitional. A vaguely bedded dark gray underclay (uc) developed between the coal seam and its clastic floor rocks. A horizon of ferrous carbonate (Fe) cuts through the lowermost section of the coal seam and runs at an acute angle with the underlying contact zone. Scale: 1-m tape meter.

tool to describe the salinity of ancient aquatic environments of deposition (Berner and Raiswell, 1984). In Fig. 15a, TOC is plotted vs. TS. Excluding two samples, which have unusually high sulfur contents, the majority of samples are enriched in carbon relative to sulfur and show a strongly positive correlation between TOC and TS. A positive correlation also exists between the TOC and C_{tot} (total carbon content) (Fig. 15b). The correlation coefficient calculated for the couple TOC–C_{tot} is much higher than for the couple TOC and TS.

4.5. Geophysical survey

The magnetic susceptibility and the gamma radiation were measured from the top of the Cretaceous (0-m level) to a depth of 100 m (Fig. 4). Sediments of lithofacies associations A and B which, at least in parts, are located in the zone of mine backfill were excluded from this survey, because field measurements of the geophysical properties, particularly the radiometry, are suspected of being impaired by the waste material dumped all around the outcrops. The readout of the gamma-radiation in log fluctuates around 200 cps and no trend or any specific correlation with a certain lithology is observed (Fig. 4). In comparison with the radiometric data, the magnetic susceptibility of the Cretaceous sediments reveals a decreasing-upward trend with some higher readings, especially, for some coarser-grained sediments. There is a negative correlation between the depth/height of profile and the magnetic properties (Fig. 4).

4.6. Palynological (kerogen analysis) and coal petrographic investigations

Palynological investigation involved quantitative and qualitative examinations of slides in which 200 particles of organic matter (phytoclasts, palynodebris) and another 100 palynomorphs were counted. The palynological results are presented in a series of composite figures, which illustrate the variation of palynomorphs in frequency diagrams and their morphology in micrographs (Fig. 16; Table 1). The palynomorphs are subdivided into different categories, each of which is characteristic of a different habitat of the parent plants (e.g., differentiation of hygrophytic and xerophytic plants, different living spaces of phytoplanktonic organisms).

Since the term kerogen, which defines the sum of all acid insoluble organic matter, has been coined by Combaz (1964), many papers have been published on this subject matter and numerous classification schemes put forward by different authors—for previous literature see Van Bergen and Kerp (1990). Our samples were classified following Van Bergen and Kerp (1990). The categorization of the palynomorphs and their environmental interpretation is based on the scheme of Visscher and Brugman (1981). It has slightly been modified and adjusted to render it suitable for Jurassic and Lower Cretaceous samples by Heunisch (1990) (Fig. 16; Table 1—see categories and legend).

Differentiation of woody phytoclasts under the microscope in transmitted light discloses internal

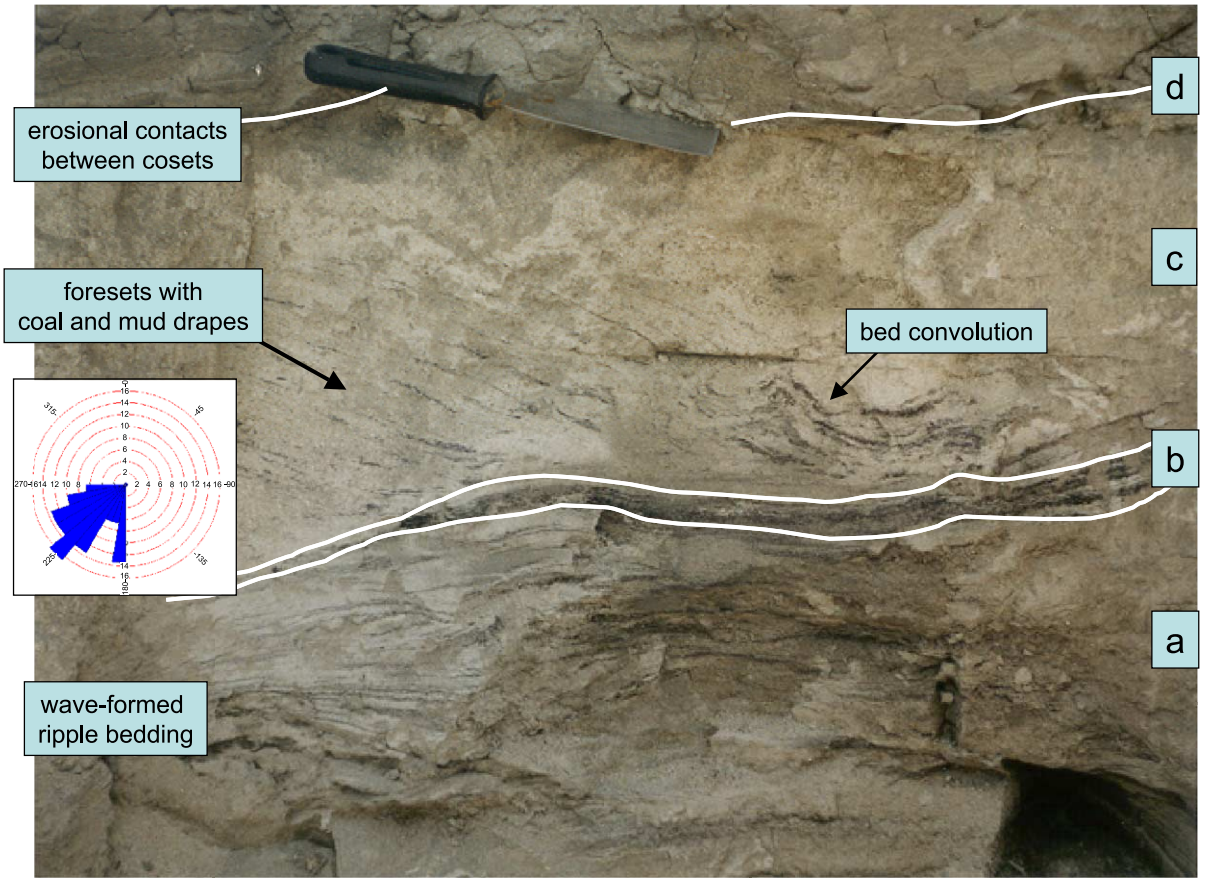

Fig. 11. Photograph showing heterolithic carbonaceous sandstones near the basis of lithofacies C. (a) The sandstone shows wave-formed ripple bedding of different dimensions (b) The coset of the lower ripple-bedded sandstone is bounded on top by an undulating wavy fine- to medium-grained sandstone abundant in coalified matter. (c) Cross-bedding of the upper heterolithic sandstone gradually developed from the underlying fine-to medium-grained sandstones "b". The rose diagram illustrates the palaeocurrent trend. (d) On top of a small-scale disconformity dark gray silty mudstones came to rest (see the spatula for scale which is 20 cm in length).

textures of tiny objects, whereas thicker ones do not and appear to be opaque. Also discrimination is difficult to achieve between black wood (inertinite) and brown wood (vitrinite) fragments. Their attribution to one or the other category is often dependent on the particle thickness, which impacts the quality of the analysis. The objects devoid of any significant properties for differentiation or seemingly amorphous were classified as structureless organic matter (S.O.M.) in Fig. 16 and Table 1. The remaining categories include objects which are well-structured and amorphous plant tissue and cuticles.

Two major categories may be distinguished among the palynomorphs. First, the category of microspores, which has been derived from ferns, sphenopsids and lycopods, is normally called hygrophytic plants (categories A–D). Second, the category pollen grains are microspores of predominantly gymnospermeous origin. For the time span concerned, gymnosperms differ from spore-producing plants independent of water. They can also settle in dry habitats (xerophytic plants). Pollen grains are prone to transport by wind and water which is the prevailing medium of transport for spores.

Reflectance measurements during coal petrographic studies yielded a vitrinite/huminite reflectance between 0.38% and 0.43%. The major maceral groups identified under the coal micro-

Fig. 12. Photograph showing medium-grained sandstones of lithofacies association F interbedded with small coal lenses (a)—see photo. The coal seams show wavy roof and nearly planar floor contacts. Height of person for scale is 1.7 m.

scope are fusinite and inertinite. Samples of detrital coal consist of phlobaphinite alternating with resinite.

Fig. 13. Photograph showing a tree trunk in growth position in a sequence of dark gray siltstones within delta plain sediments of the lacustrine delta (fine- and medium-grained sandstones of lithofacies association C).

5. Discussions

5.1. Provenance analysis of the detrital material

The lithoclast assemblage of the Lower Cretaceous sediments has been derived from two different sources. One provenance area contained acidic plutonic rocks and the other area included volcanic rocks. Sporadic vitroclastic debris among the lithoclasts are interpreted as tephra fallout that was expelled from Lower Cretaceous vent systems (Gerel, 1998; Halim et al., 1998; Badarch et al., 2002).

The abundant alkaline feldspar and smectite-group sheet silicates lend support to the idea of dual source areas of plutonic and volcanic igneous rocks. An improvement of the sorting values of the mineral fragments is related to a decrease in grain size and an improvement of roundness. Apart from depositional processes, composition also exerts control on grain size sorting. Clastic rocks abundant in primary feldspar tend to fall into a poorer sorting class than more quartzose arenites. The breakdown of feldspar into kaolinite-group minerals on weathering leaves a fine-grained (pseudo)matrix of clay minerals and a residue of quartz grains. Poor sorting is representative of epiclastic pyroclastic rocks which were primarily enriched in feldspar.

Table 3
Chemical composition of the Lower Cretaceous sedimentary rocks in the Baganuur Basin

	La	SiO_2	TiO_2	Al_2O_3	Fe_2O_3	MgO	CaO	Na_2O	K_2O	P_2O_5	SO_3	LOI	Ba	Ce	Co	Cr	Cu	La	Nb	Ni	Pb	Sn	Sr	Th	U	Y	Zn	Zr
Min	G	10.96	0.00	0.12	0.16	0.01	0.20	0.04	0.02	0.00	0.01	3.59	10	20	3	10	10	20	2	3	4	2	11	5	3	3	3	3
Mean	G	55.63	0.38	9.12	1.60	0.45	1.95	0.50	1.81	0.07	0.10	28.05	248	54	5	27	27	35	10	11	13	6	108	18	29	20	40	97
Max	G	77.91	0.98	18.98	3.60	0.98	8.14	1.83	4.20	0.18	0.36	74.95	496	129	10	56	51	76	24	28	24	12	315	47	114	48	109	217
Min	F	35.66	0.01	0.17	0.19	0.02	0.26	0.05	0.03	0.00	0.01	3.13	16	20	3	13	10	20	2	3	4	2	12	5	3	3	3	3
Mean	F	60.81	0.52	13.54	2.57	0.69	0.79	0.74	2.98	0.10	0.06	16.78	381	69	7	31	13	36	14	8	14	7	82	21	13	27	80	168
Max	F	74.10	0.90	18.09	4.06	1.09	2.12	1.30	4.18	0.19	0.20	43.48	578	106	27	42	27	61	24	29	20	16	100	34	50	42	210	317
Min	E	38.97	0.25	10.41	1.57	0.41	0.30	0.29	1.92	0.04	0.01	2.38	284	26	3	19	10	20	7	3	8	2	64	9	3	13	40	121
Mean	E	61.84	0.62	16.35	3.08	0.84	0.58	0.58	3.41	0.12	0.01	12.12	467	75	7	39	23	37	16	6	15	11	75	23	6	29	76	218
Max	E	77.19	0.89	19.69	4.41	1.17	0.79	0.82	4.80	0.18	0.03	44.26	534	100	11	55	41	48	23	10	19	16	89	32	11	36	141	305
Min	D	20.89	0.27	4.80	1.06	0.30	0.85	0.08	0.72	0.02	0.02	9.96	125	21	3	14	10	20	11	3	4	2	63	9	6	26	3	21
Mean	D	53.15	0.72	15.23	3.23	1.00	0.93	0.81	2.59	0.13	0.06	21.65	461	88	10	39	36	54	19	8	16	7	113	25	12	41	86	233
Max	D	61.23	0.90	17.70	4.15	1.34	1.00	1.23	3.08	0.19	0.23	70.38	571	128	20	60	152	79	23	18	27	13	135	32	23	53	140	304
Min	C	50.46	0.50	10.48	2.38	0.73	0.96	0.12	1.73	0.10	0.02	7.87	371	96	3	29	10	47	9	3	17	6	104	18	6	41	57	93
Mean	C	56.51	0.82	15.80	4.20	1.08	1.00	0.70	2.55	0.15	0.03	16.64	480	108	9	43	23	62	18	10	21	9	119	27	12	44	103	243
Max	C	64.49	1.02	18.64	6.57	1.40	1.08	1.41	3.14	0.21	0.04	31.82	583	134	20	69	45	77	22	25	23	12	144	34	21	47	134	478
Min	B	13.50	0.03	0.86	0.38	0.17	0.77	0.06	0.05	0.01	0.01	9.48	53	20	3	3	10	27	2	3	4	2	71	5	3	6	3	3
Mean	B	36.81	0.47	9.52	2.16	0.63	1.32	0.64	1.80	0.11	0.14	46.01	278	60	4	21	10	45	12	4	11	7	90	17	6	22	53	174
Max	B	60.12	0.91	18.17	3.94	1.09	1.86	1.22	3.54	0.21	0.27	82.54	502	99	5	38	10	62	21	5	17	11	109	29	8	37	102	344
Min	A	3.81	0.04	0.78	0.78	0.25	0.36	0.07	0.06	0.01	0.11	6.40	52	20	3	4	10	20	4	3	4	2	83	5	3	12	3	3
Mean	A	40.39	0.38	9.53	2.13	0.56	1.34	0.23	1.73	0.06	0.30	42.97	497	65	7	19	11	41	10	5	13	3	117	15	6	30	42	127
Max	A	70.58	0.91	18.06	4.07	1.07	2.51	0.66	4.13	0.12	0.71	90.27	1271	130	13	39	14	84	20	8	28	6	133	29	9	50	102	237

La (Lithofacies association). SiO_2 to LOI are given in wt.%. Ba to Zr are given in ppm.

Table 4
Correlation of element and mineral assemblages

(a) Matrix of element correlation

	Si	Ti	Al	Fe	Mg	Ca	Na	K	P	S	LOI	Ba	Ce	Co	Cr	Cu	La	Nb	Pb	Sn	Sr	Th	U	Y	Zn	Zr
Si	1.00																									
Ti	0.32	1.00																								
Al	0.50	0.91	1.00																							
Fe	0.26	0.90	0.84	1.00																						
Mg	0.26	0.95	0.90	0.93	1.00																					
Ca	−0.67	−0.20	−0.30	−0.16	−0.11	1.00																				
Na	0.55	0.37	0.58	0.30	0.37	−0.28	1.00																			
K	0.66	0.60	0.85	0.57	0.59	−0.39	0.76	1.00																		
P	0.45	0.92	0.89	0.81	0.88	−0.22	0.56	0.70	1.00																	
S	−0.79	−0.47	−0.54	−0.34	−0.39	0.56	−0.43	−0.51	−0.50	1.00																
LOI	−0.93	−0.61	−0.78	−0.55	−0.57	0.58	−0.65	−0.84	−0.70	0.78	1.00															
Ba	0.44	0.70	0.79	0.64	0.69	−0.23	0.49	0.69	0.68	−0.39	−0.65	1.00														
Ce	0.27	0.92	0.80	0.86	0.85	−0.17	0.26	0.48	0.83	−0.36	−0.53	0.66	1.00													
Co	−0.15	0.26	0.20	0.46	0.33	0.04	−0.07	0.08	0.13	0.20	0.02	0.02	0.29	1.00												
Cr	0.24	0.84	0.76	0.79	0.81	−0.17	0.14	0.44	0.65	−0.49	−0.48	0.46	0.75	0.33	1.00											
Cu	−0.06	0.15	0.15	0.14	0.22	0.14	−0.00	0.03	0.09	−0.05	−0.02	0.05	0.06	−0.02	0.24	1.00										
La	0.18	0.84	0.67	0.79	0.77	−0.10	0.18	0.32	0.76	−0.28	−0.41	0.61	0.92	0.24	0.67	0.07	1.00									
Nb	0.22	0.93	0.84	0.83	0.86	−0.18	0.32	0.55	0.81	−0.41	−0.50	0.60	0.86	0.26	0.87	0.16	0.78	1.00								
Pb	0.47	0.82	0.82	0.75	0.72	−0.27	0.49	0.66	0.79	−0.45	−0.69	0.77	0.81	0.22	0.64	−0.04	0.75	0.73	1.00							
Sn	0.38	0.73	0.76	0.71	0.70	−0.25	0.31	0.58	0.71	−0.46	−0.59	0.44	0.59	0.24	0.65	0.00	0.48	0.60	0.62	1.00						
Sr	−0.40	0.19	0.14	0.22	0.29	0.82	0.16	0.04	0.20	0.34	0.20	0.24	0.18	0.10	0.06	0.18	0.22	0.14	0.15	−0.05	1.00					
Th	0.30	0.94	0.86	0.84	0.85	−0.22	0.27	0.56	0.84	−0.43	−0.57	0.58	0.89	0.27	0.87	0.19	0.82	0.93	0.79	0.70	0.09	1.00				
U	−0.48	−0.04	−0.14	−0.02	0.01	0.90	−0.26	−0.25	−0.11	0.34	0.37	−0.18	−0.01	0.14	0.04	0.19	0.04	−0.01	−0.17	−0.13	0.71	−0.03	1.00			
Y	0.06	0.83	0.70	0.72	0.79	−0.08	0.20	0.35	0.69	−0.31	−0.32	0.49	0.83	0.22	0.72	0.16	0.75	0.80	0.62	0.47	0.27	0.78	0.04	1.00		
Zn	0.24	0.81	0.74	0.81	0.76	−0.19	0.29	0.49	0.69	−0.32	−0.48	0.52	0.85	0.55	0.74	0.08	0.71	0.81	0.68	0.53	0.09	0.81	0.00	0.68	1.00	
Zr	0.49	0.80	0.83	0.64	0.77	−0.28	0.65	0.72	0.88	−0.49	−0.70	0.71	0.71	−0.01	0.52	0.11	0.60	0.73	0.69	0.61	0.14	0.69	−0.21	0.62	0.59	1.00

(b) Element couples of correlation coefficients $r>0.75$

Phyllosilicates	Ti	Al	Fe	Mg	Cr				
	Fe	Mg	Cr	Al	Ti	Nb	Sn		
	Mg	Ti	Al	Fe	Cr	Nb			
	K	Al							
	Ba	Pb							
	Ti	Pb	Zn						
	Mg	Zn							
	Zn	Ti	Fe	Mg	Nb				
Phyllosilicates and heavy minerals	Al	Fe	Mg	K	Ba	Cr	Nb	Sn	Zr
	Th	Al	Fe	Mg					
	Al	Ce	Th	Y					
	Zr	Mg							
Heavy minerals	Ti	P	Ce	La	Nb	Sn	Th	Y	Zr
	Fe	P	Ce	Th	La				
	P	Ce	La	Nb	Th	Zr			
	Th	Ti	Ce	La	Nb				
	Zn	Ce	Th						
	Zr	Ti	P						
Suphur bound to organic matter and sulphides	S	C							
Duricrusts (uraniferous)	Ca	Sr	U	<C	<S				
Alkaline feldspar	Na	K							
Aluminum phosphates	P	Pb							
	Fe	Pb							
	Al	Pb	Zn						
	Al	P							

The heavy mineral suite contains only a few minerals that may be used as marker to interpret the source area. Sphene and epidote originated from the breakdown of (meta)basic igneous rocks, whereas monazite and stubby apatite are typical of acidic igneous. Brookite and anatase resulted from chloritisation of biotite. Pyroclastics and volcanic rocks subject to hydrothermal alteration are well known to provide such a heavy mineral assemblage (Kemper and Zimmerle, 1982). A significant proportion of

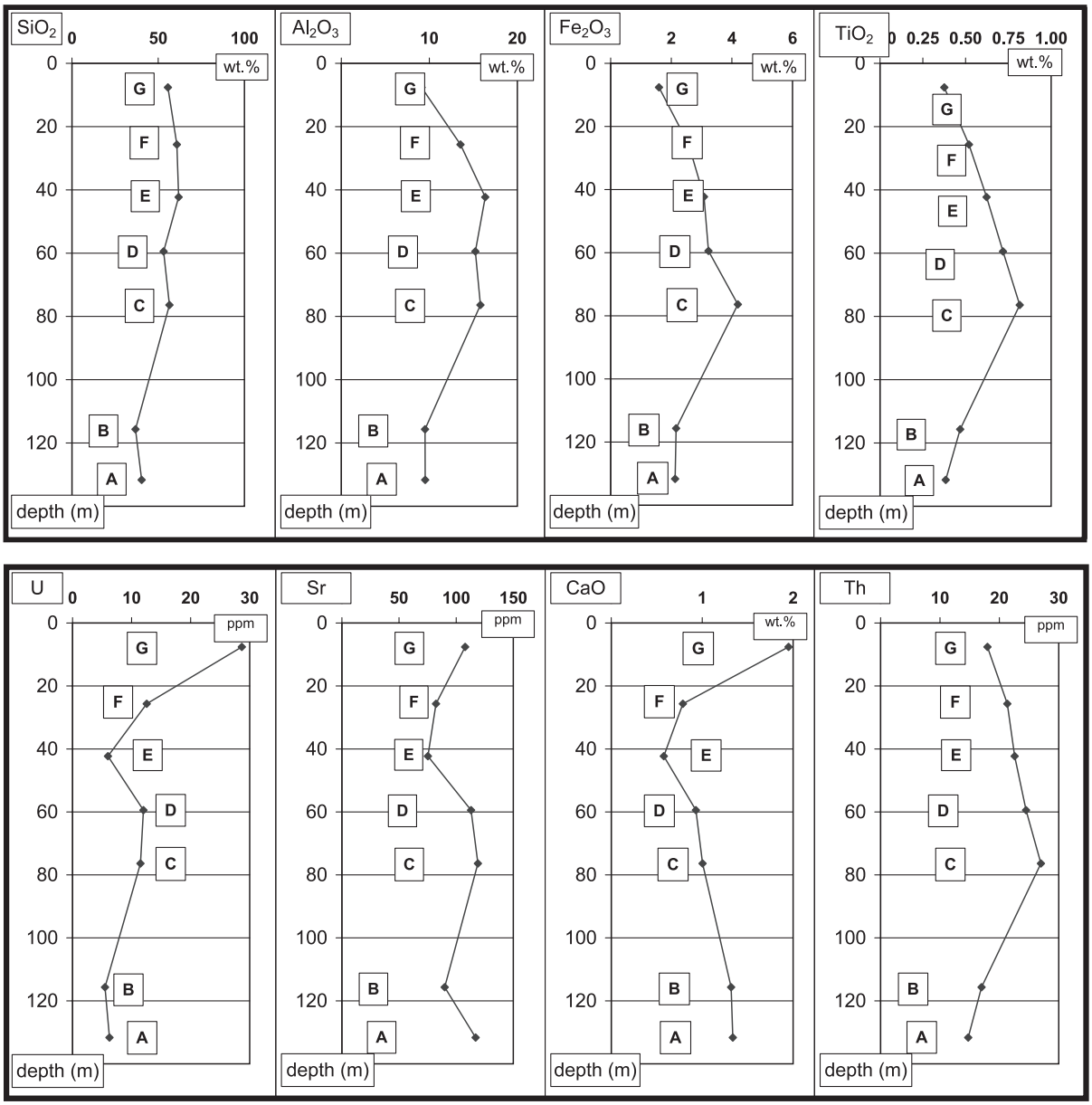

Fig. 14. Chemologs of the Lower Cretaceous sedimentary rocks of the Baganuur Basin. The depth-related plots show the mean values of major elements (Si, Al, Fe, Ti, Ca) and trace elements (U, Sr, Th, Cu, Zn, Co, Ni, Zr) (see also Table 1). The capital letters in the squares denote the lithofacies associations which were referred to in the text.

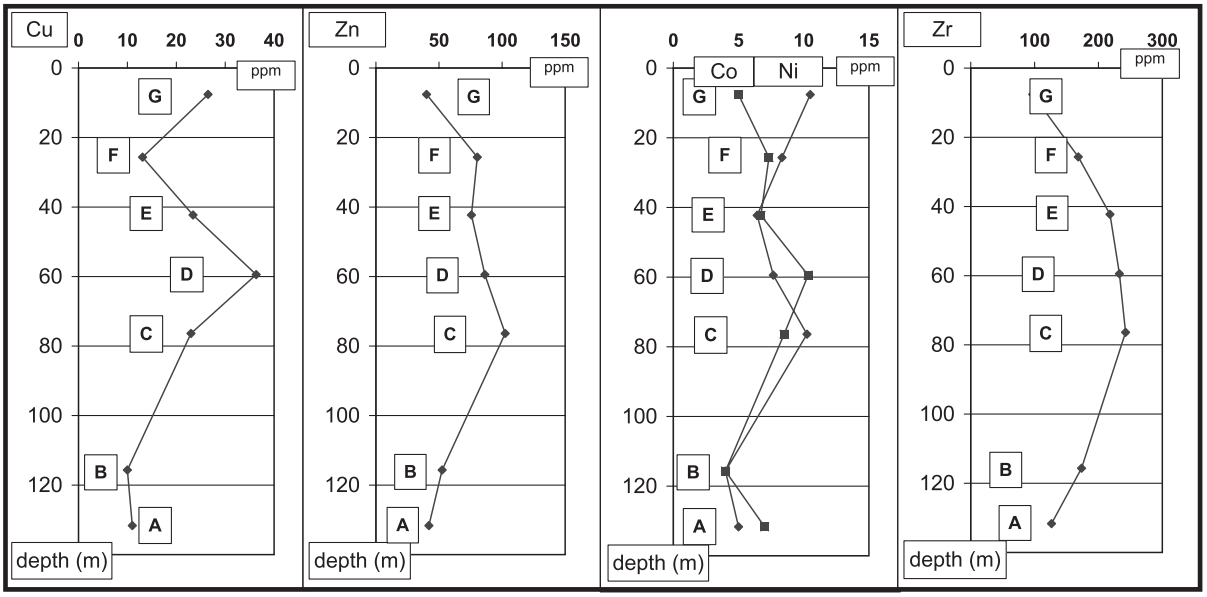

Fig. 14 (*continued*).

heavy minerals including the ultrastable silicates zircon and tourmaline is recycled. Garnet considered resistant to weathering and diagenesis originated from medium-grade regionally metamorphosed crystalline rocks. The association of heavy minerals of different stabilities may be explained by heavy mineral mixing derived from different sources rather than differential alteration by meteoric waters.

Considering the chemical composition, the good linear correlation between P, Th, Zr, Ce and Y provides convincing evidence that rare-earths-elements-bearing phosphates (e.g., monazite) are present in the Lower Cretaceous rocks. Zirconium is unequivocally the most appropriate marker element for the heavy minerals in these siliciclastic rocks (Dill, 1998). The good correlation of Ti, Sn and Nb is another evidence for the presence of some brookite and anatase in the heavy mineral assemblage. Hydrothermal alteration which has brought about the TiO_2 modifications is likely to have taken place in a granitic provenance area, which have contributed the accessory minerals monazite and zircon. The coupling of Th, Zr, Ce and Y with major element such as Al, Ti and Mg indicates a close spatial and genetic association of phyllosilicates with heavy minerals. Both mineral groups are interpreted to have been derived from the same acidic parent material.

5.2. Uplift, basin subsidence and transport of detrital material

The alternating FU and CU sequences observed in the Lower Cretaceous basin fill reflect changes from fluvial-dominated environments with channel-fill deposits to progradational delta-dominated environments. This is supported also by the variation of cross-stratification. Trough cross-stratification is widespread in the fluvial channel deposits, whereas planar cross-stratification is more common to deltaic deposits. Flaser-bedding is not interpreted here in terms of tidal origin as it was done by Reineck and Singh (1980), but held to be indicative of a lower flow regime and settling out of suspension. Stagnant waters where the current was almost nil are represented by concentrations of organic matter and fine-grained sediments (Fig. 6). Such changes may illustrated in their best by the chemologs and physical logs (Figs. 4 and 14).

The distributions of Si, Al, Ti and Fe are controlled by the quantities of phyllosilicates and framework silicates present in the terrigenous sediments (see also Section 5.1). Judging by the chemologs in Fig. 14, the detrital influx into the basin became reduced during periods when organic matter was increasingly laid down in lacustrine deposits or accumulated in swamps. Concluding from these logs, an abrupt

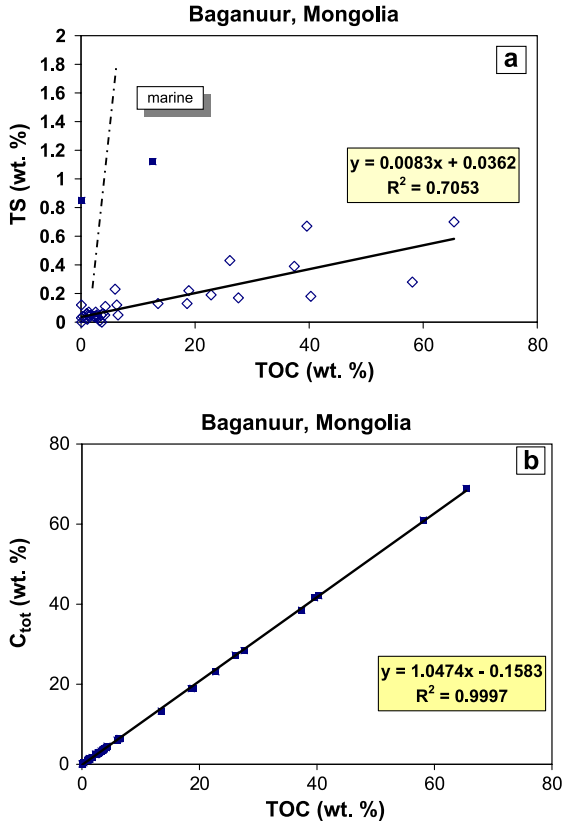

Fig. 15. Plots showing relationship of organic chemistry of the Lower Cretaceous sedimentary rocks of the Baganuur Basin. (a) Total sulfur content (TS) plotted vs. total organic carbon content (TOC) with regression line and correlation coefficient. The stippled line denotes the C/S ratio indicative of marine sedimentary rocks (e.g., Berner and Raiswell, 1984). The full squares were not considered for correlation. (b) Total organic carbon content (TOC) plotted vs. total carbon content (C_{tot}) with regression line and correlation coefficient.

increase in the rate of sedimentation occurred in lithofacies association C when a delta began prograding onto lacustrine deposits of lithofacies association B. The amount of detritus and the lithological variation excludes the presence of crevasse splays in this part of the litholog (Fig. 6). The pronounced variation in the chemical composition is a direct response to the vertical uplift and unroofing in the hinterland and triggered delta progradation in the intermontane basin (Figs. 6 and 14).

The heavy minerals also attest to an increasing rate of uplift in the source area by the beginning of lithofacies association C. Zirconium and thorium, found in the heavy minerals zircon and monazite, have distribution curves quite similar to those of Al, Ti and Fe, illustrating an exceptional accumulation or "placer like" concentration of accessory minerals during delta progradation in lithofacies association C (delta progradation is the first-order process of deposition, fluvial aggradation the second-order process of deposition).

Trends in the detrital input may be deduced from the variations of the magnetic properties and natural gamma radiation. The scintillometer enables us to distinguish host rocks abundant in K-bearing silicates and/or Th- and U-bearing heavy minerals from those sections depleted in these minerals. No increasing- or decreasing-upward trend correlated to tectonic pulses or any step-like uplift of a granitic rocks area can be observed (Section 4.3) (Fig. 4). The magnetic susceptibility of the sedimentary rocks are a direct response to the amount of magnetite present in the rock. Pyrrhotite can be ruled out in this continental terrigenous environment of deposition and under the present conditions of post-depositional alteration (Zeman, 1989; Tuttle and Goldhaber, 1993). Magnetite is abundant in coarse-grained fluvial sediments of lithofacies associations C, D and E. The Fe oxide, which is very stable and not highly susceptible to weathering and attrition throughout transport, was used as a measure of the amount of basic detrital material deposited into the basin.

5.3. Physico-chemical conditions during deposition of the coal-bearing series

The rock color may provide a first-hand information on the redox conditions. Gray and black shades found all across the entire basin attest to aquatic reducing conditions. Long-term periods of emersion during deposition did not occur in the coal-bearing intermontane basin. The strong positive correlation of sulfur and organic carbon is indicative of S associated with organic matter (Table 4; Fig. 15). This coupling, however, does not tell us anything about the bonding of sulfur (Boudou et al., 1987). Ore microscopy reveals that pyrite is the major host of sulfur in Baganuur. Since there is no correlation between base metals and sulfur, a simple model of coprecipitation of Cu, Zn, Pb and S to form chalcopyrite, sphalerite or galena cannot be applied to the rocks under study.

Therefore, the sedimentary environment may by characterized as slightly reducing or dysaerobic. There was obviously only little bacterially produced sulfur available throughout most of the time of deposition.

The chemologs of Pb and Zn resemble the distribution curves of Ti, Al or Fe which reflect the detrital input into the basin (Fig. 14). Accordingly, Pb and Zn are thought to be bound to phyllosilicates rather than forming sulfide minerals on their own. The concentration of Cu, Ni and Co was very much different from that of the Pb and Zn. Their down-hole plots neither correlate with those of other base metals nor do they show any relation to major element. Cu, Ni and Co concentrations are independent of the detrital accumulation in the basin. The chalcophile elements which are slightly enriched in lithofacies associations C and D are present in the lattice of some Fe disulfides or bound to organic matter. They are present only in small amounts.

Besides minor pyrite, siderite is the only authigenic mineral which hosts bivalent iron in the carbonaceous layers and coal seams. Under suboxic to anoxic conditions, ferric hydroxide may be converted to siderite. Siderite may also be used as a geo-acidometre. This ferroan carbonate precipitates in the pH range 7 to 9 and at Eh values down to −0.4 V in the system Fe–O–C–H at 25 °C and 1 bar (Brookins, 1988; Jakobsen, 1988; Virtanen, 1994; Lensing et al., 1995).

Aluminum, phosphorous, iron, lead and zinc are positively correlated. Presumably, aluminum–phos-

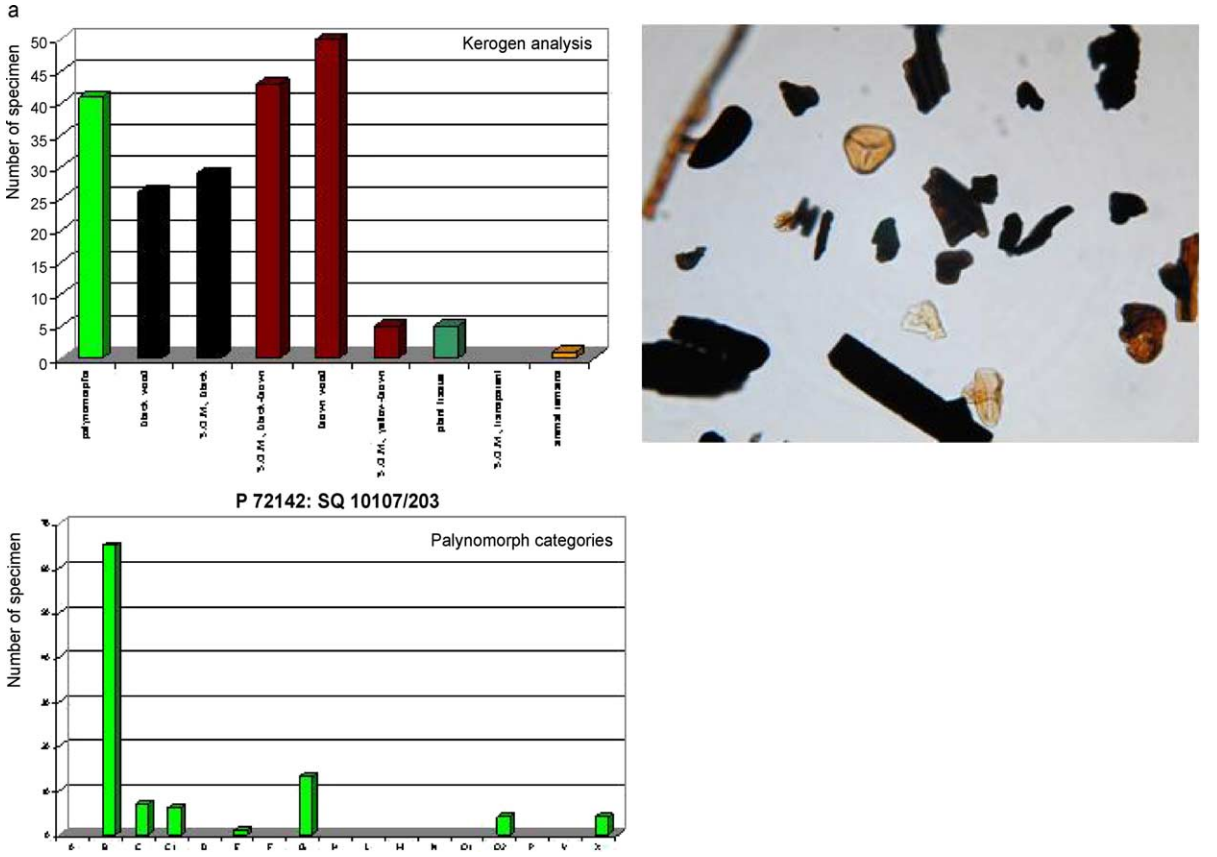

Fig. 16. Frequency diagrams of palynological data of the Lower Cretaceous sedimentary rocks of the Baganuur Basin. (a) Tuffaceous siltstone to fine sand with plant debris (No. P 72142—SQ 10107/203). For explanation of the categories see Table 1b. (b) Fine- to medium-grained sandstone with plant debris (No. P 72139—SQ 10107/162). For explanation of the categories see Table 1b. (c) Siltstone (No. P 72143: SQ 10107/53) For explanation of the categories see Table 1b.

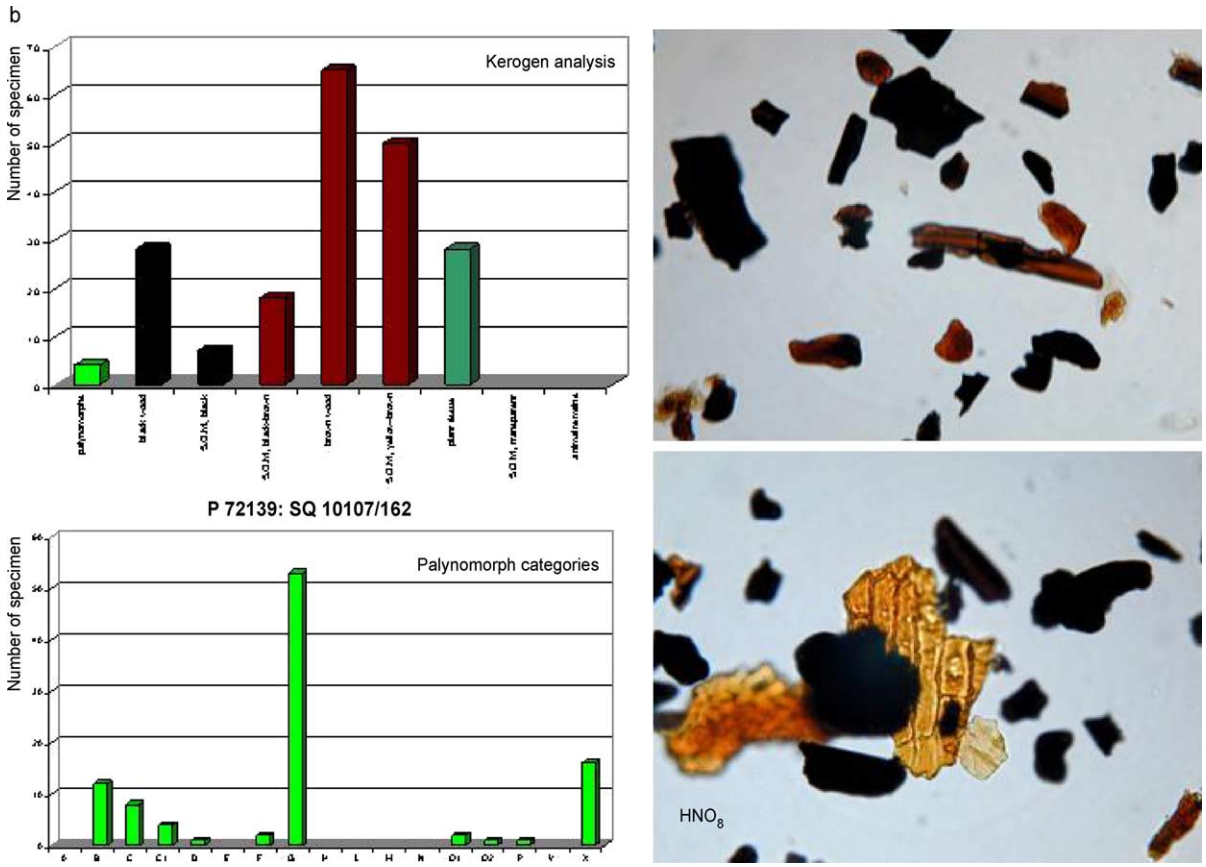

Fig. 16 (*continued*).

phate–sulfate minerals (APS minerals) are present in minor quantities. APS minerals are mostly dispersed in the matrix of rocks so that highly sophisticated measurements are necessary to guarantee good results during mineral identification (Dill, 2001; Dill and Pöllmann, 2002). The depositional setting is favorable for APS minerals to come into existence in the carbonaceous layers. Ward (1978), Reinink-Smith (1990), Bohor and Triplehorn (1993), Rao and Walsh (1999) reported abnormally high P_2O_5 contents from Alaskan coals of the Cook Inlet interbedded with tonsteins. Most of the phosphorus contents were ascribed to APS minerals of the goyazite–crandallite solid–solution series. Stability field of apatite is reduced at the expense of APS minerals when the pH is lowered. Conditions favorable for the precipitation of APS minerals occurred only in some coal swamps with a pH in the range 3.3–4.6.

The pH values of the pore fluids were subject to some changes throughout basin subsidence. Kaolinite forms in acidic pore solutions, whereas phyllosilicates of the smectite-group can only be preserved under alkaline conditions. The association of unstable heavy minerals with ultrastable minerals does not allow strong diversions of the pH of intrastratal solutions towards either strongly acidic or alkaline conditions. This is also proven by the persistence of kaolinite-, smectite- and mica-group minerals in the same host rock. These physico-chemical data indicate an absence of a strong chemical weathering under tropical or subtropical climatic conditions in the study area.

The salinity of the basin is deduced from the TS/TOC ratio and the palynological data, both of which point to a true freshwater environment or, in other words, to perennial lakes in an alluvial plain or floodplain. In comparison with TOC, the TS is very

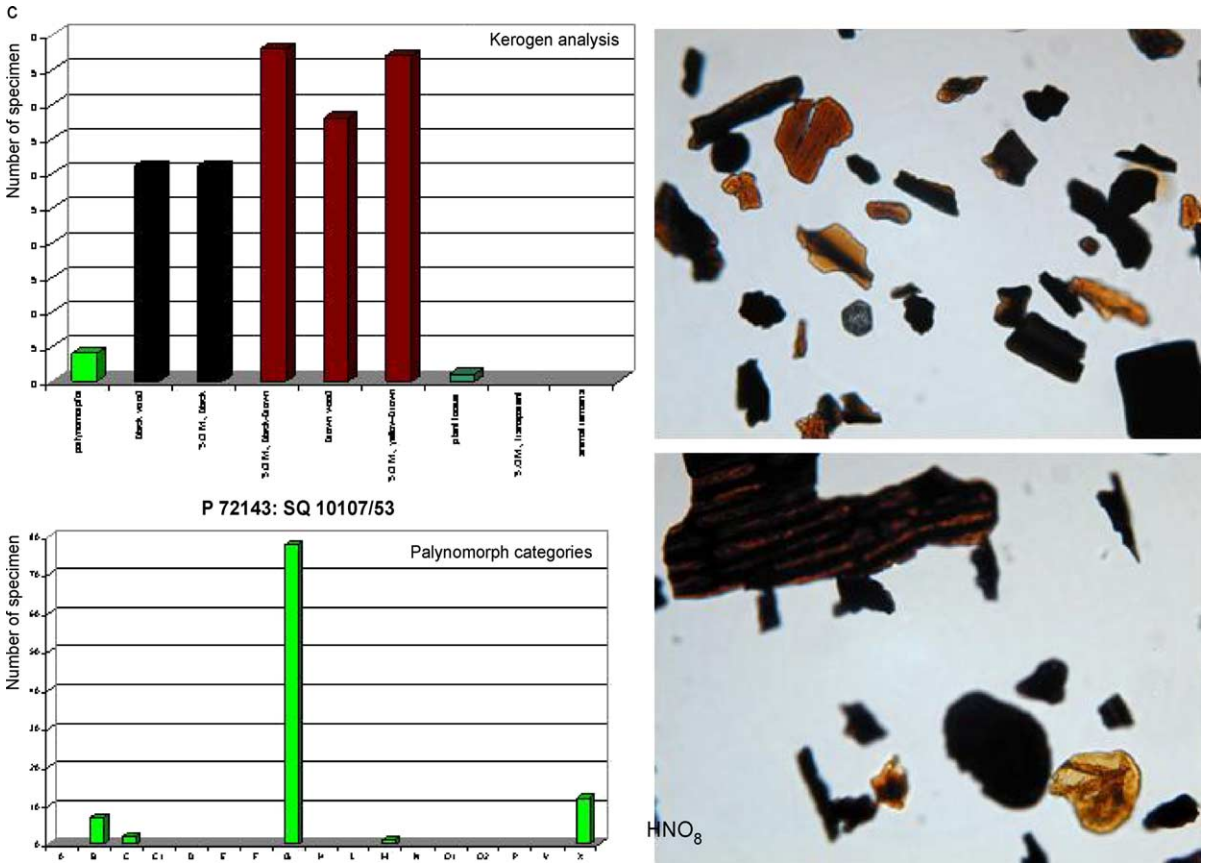

Fig. 16 (*continued*).

low with TS values of as high as 0.9 wt.% S (Fig. 15a). Sulfur/carbon ratios are largely applied to discriminate freshwater and marine environments (Berner, 1997; Berner and Raiswell, 1984; Morse and Berner, 1995; Berner and Petsch, 1998; Dill et al., 2002). Sediments from freshwater lakes are low in sulfur as sulfate reduction plays only a minor role in the transformation of the organic matter. The TS vs. TOC cross plot, apart from two samples clustering outside the field, indicates typical non-marine environments of deposition (Berner and Petsch, 1998) (Fig. 15). TS and TOC display a positive correlation that corroborates the idea of sulfur to be bound to organic matter and Fe disulfides (Fig. 15a). For the pair TOC and C_{tot}, a correlation coefficient of $r^2 = 0.99$ was calculated, based on 30 samples. Due to this significant correlation, the presence of carbonate minerals in the rocks is considered to be negligible. Only some siderite nodules were encountered in the carbonaceous beds (Fig. 10).

5.4. Diagenesis and coalification

The coal rank may be determined petrographically as lignite to subbituminous C. Diagenetic to epigenetic alteration of the interseam sediments is less easy to identify.

The distribution curves of Ca, U and Sr reach a maximum in lithofacies association G and a minimum in lithofacies association E (Fig. 14). Chemical residues substantially increased in stagnant bodies of water and in swamps, whereas fluvial and deltaic depositional systems (lithofacies association E) are considerably deprived of precipitates containing Ca, U and Sr. The relative minimum in the distribution curves of Ca, U and Sr for lithofacies association E

reflect either a low rate of precipitation during early diagenesis or a high rate of dissolution of these elements during late diagenesis. Lithofacies association E consists of a stagnant or quiescent water lithofacies. The lithofacies is abundant in potential reductants, underlain and overlain by a highly transmissive lithofacies assemblage of fluvial deposits. The physicochemical conditions are favorable for element precipitation as well as groundwater-related redeposition. A small-scale redistribution of U similar to what is recorded from roll-front deposits elsewhere may be envisaged for the Neocomian hydrologic system (Galloway and Hobday, 1996). The distinctive geometry of the lithofacies association in the Lower Cretaceous rocks, the alternation of transmissive and sealing horizons, and the chemical zonation within these units suggest that at least part of the Ca, U and Sr have been remobilized from the floor rocks (lithofacies association E) and precipitated in the uppermost stratigraphic column (lithofacies association G) as the uppermost interseam sediments were brought into the reaches of a post-Lower Cretaceous hydrological system. This re-deposition took place under a high aridity condition. Brown and reddish shades in the rock color, which were exclusively found on the uppermost benches in the open pit, provide evidence for post-depositional redeposition.

6. Interpretations of the depositional Environments

6.1. Biofacies of the basin fill

The organic matter observed in the Baganuur Basin originated from higher plants that are most likely terrestrial. Judging by the palynodebris and the palynomorph fraction, there is no evidence for marine or even lagoonal or brackish environments. Three depositional environments can be distinguished: swamp, fluvial and transitional environment. This environmental differentiation is mostly based on the variable amounts of spores and pollen grains. The swamp-related assemblages are characterized by elevated contents of spores representative of the flora which are adapted to humid conditions. These spores constitute more than 30% and reach a maximum of 72% in sample P 72142 (Fig. 16a). In the transitional environment, the number of mostly bisaccate pollen grains increased at the expense of the amount of spores (Fig. 16b—P 72139). The fluvial channel systems in Baganuur are characterized by elevated contents of bisaccate pollen grains of as much as 78% in P 72143 (Fig. 16c), which can be transported by wind and water. Spores are restricted to few specimens.

The fluvial–swamp environment determined from the paleoecological analysis may be refined by a closer look at the various lithofacies associations.

6.2. Lithofacies association A (fluvial–swamp)

The vertical grain size profile of Fig. 6A displays 3 FU sequences (cycles I, II and III) which are representative of meandering fluvial channel systems (Figs. 6A and 9b; Table 2). They have channel lag deposits at the base and end up in finer-grained siliciclastics on top. Their palaeocurrent pattern shows a unique trend directed towards the SW (Fig. 9b). In cycle I the floodplain/overbank deposits were truncated by the succeeding flood of cycle II, as evidenced by the absence of a fine-grained topstratum in the FU sequence of cycle I. Trough and tabular cross-stratifications are common and corroborate the interpretation of a meandering fluvial channel systems (Table 2). The FU sequences are thickening upward and, hence, bear evidence of the accommodation space to increase from cycle I towards cycle III. The main coal seam attests to a poorly drained (back) swamp that evolved from the floodplain deposits of the uppermost point-bar sequence. A gradual downcurrent variation of the textural maturity may be observed from cycle I to cycle III. Within each of the three fluvial cycles, the roundness of grains and the sorting of the sedimentary rocks improved as the fluvial drainage system entered the swamps.

The peculiar situation at the contact between the floor rock and the seam in lithofacies association A cannot be deduced from the litholog of Fig. 6A. Fig. 8 demonstrates that the fluvial deposition caused a local seam splitting and truncation of the bed. The causes for the seam splitting are autocyclic in which the fluvial channels encroached into the swamp. The clastic wedge pinches out into a bright gray ash band that records a break in peat accumulation as a result of flooding of the swamp.

Ash bands in the coal seam may record breaks in peat accumulation as a result of factors such fire (Scott, 2000; Scott and Jones, 1994). Fine banding on a centimeter to decimeter scale represents an alteration of bright and dull laminae which consists of different coal lithotypes.

6.3. Lithofacies association B (fluvial–lacustrine)

The grain size profile in lithofacies B is not very much different from the stacked fluvial cycles in lithofacies association A (Fig. 6B). Here the fluvial cycles are interpreted as an anastomosing rather than a meandering fluvial channel. The paleocurrent pattern calculated from field data is polydirectional (Fig. 9b). Sheet sands common to lithofacies association B are evidence for this interpretation. In contrast to lithofacies association A, subsidence of the basin and provision of accommodation space, however, were faster than in previous lithofacies association so that accumulation of organic matter in poorly drained swamps could not keep pace and the peat eventually drowned (Fig. 6B). The ratio of siliciclastics/coal is much higher in lithofacies association B than in lithofacies association A (Table 2).

The multistoried channel sandstones with convex bounding surfaces and gently dipping foresets are due to lateral channel migration and erosion (Fig. 8; Table 2). The southwestward dipping beds highlighted in Fig. 11 are a direct response of a mixed-load channel deposition which caused the FU successions. In the fluvial FU cycles, the finer-grained sandstones are interpreted as overbank fines. The fluvial environment was gradually replaced by a lacustrine environment. Splitting of overbank fines is due to encroachment of distributary channel sands or crevasse splay deposits onto the overbank sediments. Differential compaction in the underlying organic matter and an overall basin subsidence led to variation in grain size and change in the bedding geometry with a steepening of foresets.

6.4. Lithofacies association C (deltaic–fluvial)

A conspicuous facies change may be inferred from the chemologs and lithologs at the passage from lithofacies association B to C (Figs. 6 and 14). Extrabasinal processes responsible for an increase in the supply of detritus were superimposed on intrabasinal processes. Fine-grained horizons with comminuted plant material are representative of swamps. A CU trend during the initial stages of lithofacies association C heralds the progradation of a fluvial-dominated delta onto degraded swamps/siliciclastic lacustrine deposits. The overall features of the bedforms are indicative of fluvial–deltaic depositions with all the hallmarks of the prodelta to delta plain environments (Fig. 6C; Table 2). Deposition took place in a distal position, as indicated by parallel and tabular cross bedding in the fine-grained sedimentary successions with channels and trough cross bedding being absent. Channeling and trough-shaped cross-bedding appear higher up in the stratigraphic section, in the coarser-grained sandstones which were interpreted as distributary channels, levees and crevasse splays (Fig. 6C). The dip direction of foreset beds was measured in the field. The data obtained throughout these field measurements point to a general paleocurrent oriented towards the SW. In the lower part of lithofacies association C the environment of deposition is transitional between a (storm)-wave-dominated (a–b) and a current-dominated environment (c) (Fig. 11). The bundles of sand and organic matter reflect a variation of deposition from suspension and oscillating flow of waves (Fig. 11). The sedimentary structures resemble hummocky cross-stratification formed by storm processes (Yagishita et al., 1992; Amos et al., 1996; Ishigaki and Ito, 2000; Ito et al., 2001; Begossi and Della Fávera, 2002). Rather clean and monotonous coarse-grained arenaceous sediments are characteristic of the distributary mouth bar and delta plain deposits which came to rest on top of dark-colored lacustrine prodelta deposits. The close similarity between these near-shore lacustrine/deltaic sedimentary rocks of lithofacies association C and near-shore-marine deposits is indicative of similar hydrodynamic processes which took place in lithofacies association C. This does not imply any marine influence on the environments under study (see palynology).

Tree trunks in growth position and drift wood are widespread in the distributary channel, levee and crevasse splay deposits (Fig. 13). The water depth of the interdistributary bays is interpreted to have been from 2 to 3 m, based upon the size of the tree trunks. For a certain period of time, growth of trees was able to keep pace with rising water level. The water depth

of the interdistributary bays is supposed to have rapidly increased, exceeding that of what has been estimated for the tree trunks in Fig. 13 (>3 m), which were drowned by catastrophic floods. The trees were broken and their remains silted up by crevasse splays or drifted by flash floods.

6.5. Lithofacies association D (fluvial)

Grain size variation and sedimentary structures at the boundary between lithofacies associations C and D correspond to structures transitional from a fluvio-deltaic to a fluvial regime (Fig. 6D). Ripple-laminated and rhythmically bedded units of silty clays, silt, and fine sand are typical of levees and crevasse splay deposits. They are part of the waning delta plain deposition. Sheet sands up to several hundred meters wide and as much as 10 m in thickness were probably deposited by anastomosing rivers. Such laterally extensive ribbon or sheet sands are diagnostic for anastomosing fluvial drainage pattern (Makaske, 2001). The paleocurrent pattern of the channel system, which was obtained from measurements of the dip direction of foresets in the field, directed towards the SE. Fining-upward sequences with some coal particles in their topstratum are evidence for a highly meandering channel facies. The fluvial system is represented by distal splay and unconfined depositional processes rather than typical channel deposits. Reworking of backswamp sediments led to chips of coal and plant debris to be scattered in the arenaceous host sediments.

6.6. Lithofacies association E (fluvial–deltaic–lacustrine/floodplain (?))

Lithofacies association E represents a transition from the fluvial to deltaic environment of deposition (Fig. 6E). The lacustrine facies intermediate to the fluvial and deltaic environment is a bit "undernourished" relative to the over- and underlying fluvial and deltaic lithofacies types. This fine-grained facies is made up of coal-bearing claystone (Fig. 6E). Therefore it does not reproduce well in the litholog (Fig. 6E) or cannot be identified in the chemologs, namely in those graphs reflecting the detrital influx into the basin (Fig. 14). It mirrors a period of starved basin or condensed sedimentation. There may also be an interpretation of this fine-grained facies as a floodplain facies rather than lacustrine (R.M. Flores, personal communication). The textural and structural criteria and the facies sequence allow for both environmental interpretations.

6.7. Lithofacies association F (lacustrine–deltaic–swamp)

Lithofacies association F has much in common with the lithofacies described in lithofacies association C. In contrast to the monophase deltaic evolution from fine-grained prodelta sedimentation to coarser-grained distributary channel deposition in lithofacies association C, the lithofacies association F represents deltaic formation alternating with deltaic abandonment or deltaic retreat (Fig. 6F). The fluvial–deltaic to fluvial regime is characterized by distal splay deposits which grade into poorly drained swamps that, locally, created thin coal seams in a delta plain environment. The crevasse splay deposits are recognized by fine- to medium-grained sand sheets. Minor channels, with channel lags grading through coarse-grained sandstones into finer-grained topstrata and the aforementioned crevasse splays encroached upon swamps, which are represented by claystones bearing lenses of coalified matter. The mat of dead vegetation could not be preserved as peat due to this episodical detrital influx and the lack of accommodation space. Rapid alternation of detrital accumulation and growth of swamps created autocyclic processes in which seam split and prevented mineable coal seams to develop in the same way as in lithofacies G and A.

6.8. Lithofacies association G (swamp–fluvial)

Lithofacies association G duplicates lithofacies association A with regard to the environment of deposition, but not with respect to size and coal quality (Fig. 6A,G). At the base of lithofacies association G, three FU successions, each starting with coarse-grained sandstone and basal channel lags and getting more abundant in organic matter, are representative of the incipient stages of fluvial deposition. Such cross-bedded FU sequences with scoured bases are typical of high-sinuosity channels and are here termed as distributary channel I through III (Miall, 1996). The depositional setting of lithofa-

cies association G, however, seems to be more distal relative to the provenance area and less prone to the accumulation and preservation of organic matter than the fluvial–backswamp environment in lithofacies association A. Subsidence was very much retarded relative to lithofacies association A and did not provide favorable paleogeographic conditions for the organic matter to develop thick and extensive swamps.

A paleosol horizon (underclay) at the base of the coal seam was recognized by the extensive rooting which led to a homogenization of the clay and silt in the horizon. Due to the lack of tree trunks found in growth position in the paleosol underlying the Upper Coal Seam, the coal seam is interpreted as semi-autochthonous with accumulation of organic matter in poorly drained swamps (Fig. 13). A rain of organic material from the underside of floating mats (floatants) settling on the lake floor as gyttja may have significantly contributed to the build up of the seam. A personal view of floatants in the Mississippi Delta by the senior author has led to this interpretation. This was also proposed by Austin (1979) for a coal in western Kentucky. It is a hypothesis which needs further clarification. A concretion horizon in the basal coal seam marks a paleoaquifer that developed during subsidence of the peat bog.

7. Conclusions

The Baganuur Basin formed along with rift or pull-apart processes during the Late Jurassic (?)–Early Cretaceous which saw several basins to evolve in eastern Asia (Yi et al., 2002). The coal measures formed in a lacustrine–fluvial environment with climates ranging from semi-arid to warm temperate. Peat accumulation is supposed to have started earlier in Baganuur than in many of the stratigraphically equivalent basins, where deposition of organic matter began as early as Barremian (Sha et al., 2002; Yi et al., 2002).

During the Berriasian, peat accumulation began in the Bagannur Basin, Central Mongolia. The palynoflora is akin to the Siberian palynological province. Based upon the phytoclast assemblages of organic sediments and the TS/TOC ratios of siliciclastic interseam sediments marine transgressions into the freshwater environment may be ruled out for the intermontane basin under consideration. Strong chemical weathering, which could create thick saprolite or even laterites, did not occur on the dry land. Sedimentation happened mostly under neutral to slightly alkaline conditions. Suboxic to anoxic conditions persisted during the Lower Cretaceous in the basin. Long-term periods of emersion did not exist.

The basin fill has been subdivided into seven lithofacies associations (A: fluvial–swamp, B: fluvial–lacustrine, C: deltaic–fluvial, D: fluvial, E: fluvial–delta lacustrine/floodplain (?), F: lacustrine–deltaic–swamp, G: swamp–fluvial). A conspicuous change in this accelerating and decelerating flow regime and in the sediment supply may be observed at the boundary between lithofacies associations B and C. Extrabasinal forces triggered the onset of delta sedimentation. Lithoclasts, heavy minerals and phyllosilicates bear witness of a mixing of detrital material rather than a differential alteration of sedimentary rocks by meteoric waters. One provenance area was abundant in acidic plutonic rocks the other source area affected by volcanic processes which produced the vitroclastic debris deposited as tephra fallout in the basin. Apart from coalification post-depositional alteration is scarce. The uppermost sediments laid down in the Baganuur Basin were brought into the reaches of post-Lower Cretaceous hydrological systems and diagenetically altered. Favored by a distinctive facies association of transmissive and sealing horizons, Ca, U and Sr underwent re-deposition.

Acknowledgments

We would like to express our thanks to E. Dagvadorj and L. Weiland for their assistance in the field and to the staff members of the Baganuur Coal Mine who gave access to the open pit for investigation. All Mongolian colleagues from the technical team have contributed very much to the success of our field trips in the Baganuur area as it was the interest in our study by the project coordinator B. Begzsuren and by O. Gerel, Head of the Department of Geology and Mineralogy of the Mongolian University of Science and Technology. Chemical analyses were carried out in the laboratory of BGR under the conductance of U. Siewers and H. Wehner. Some XRD analyses were performed in the laboratory of BGR by R. Dohrmann.

Coal petrographic investigations and measurements of vitrinite reflectance were carried out by W. Hiltmann (BGR). The project was supported by the Ministry of Development and Technical Cooperation of the Federal Republic of Germany. We acknowledge with thanks the helpful comments made to a previous draft by R.M. Flores and by C.R. Fielding who took over the review for the *International Journal of Coal Geology*. We are also grateful to J.C. Hower for editorial handling of this paper.

References

Amos, C., Li, M.Z., Choung, K.S., 1996. Storm-generated, hummocky stratification on the outer-Scotian Shelf. Geo-Marine Letters 16, 85–94.

Austin, S.A., 1979. Depositional environment of the Kentucky No. 12 coal Bed (Middle Pennsylvanian) of Western Kentucky, with special reference to the origin of coal lithotypes. PhD thesis, The Pennsylvania State University, University Park, PA. 390 pp.

Badarch, G., Cunningham, W.D., Windley, B.F., 2002. A new terrane subdivision for Mongolia: implications for the Phanerozoic crustal growth of Central Asia. Journal of Asian Earth Sciences 21, 87–110.

Bechtel, A., Gratzer, R., Sachsenhofer, R.F., 2001. Chemical characteristic of Upper Cretaceous (Turonian) jet of the Gosau Group of Gams/Hieflau (Styria, Austria). International Journal of Coal Geology 46, 27–49.

Begossi, R., Della Fávera, J.C., 2002. Catastrophic floods as a possible cause of organic matter accumulation giving rise to coal, Paraná Basin, Brazil. International Journal of Coal Geology 52, 83–89.

Benton, M.J., Shishkin, M.A., Unwin, D.M., Kurochkin, E.N., 2000. The Age of Dinosaurs in Russia and Mongolia. Cambridge Univ. Press, Cambridge. 696 pp.

Berner, R.A., 1997. The rise of plants and their effect on weathering and atmospheric CO_2. Science 276, 544–546.

Berner, R.A., Petsch, S.T., 1998. The sulfur cycle and atmospheric oxygen. Science 282, 1426–1427.

Berner, R.A., Raiswell, R., 1984. C/S method for distinguishing freshwater from marine sedimentary rocks. Geology 12, 365–368.

Blair, T.C., McPherson, J.G., 1999. Grain-size and textural classification of coarse sedimentary particles. Journal of Sedimentary Research 69, 6–19.

Boersma, J.R., van Geldern, A., De Groot, T., Puigdefabregas, C., 1981. Formen fluviatiler Sedimentation im Braunkohlentagebau Frechen (Niederrheinische Bucht). Fortschritte in der Geologie von Rheinland und Westfalen 29, 275–307.

Bohor, B.F., Triplehorn, D.M., 1993. Tonsteins: altered volcanic-ash layers in coal-bearing sequences. Special Paper-Geological Society of America 285, 1–5.

Boudou, I.P., Boulegue, I., Malechanx, L., Nip, M., de Lluw, I.W., Boon, I.I., 1987. Identification of some sulphur species in a high organic coal. Fuel 66, 1558–1569.

Brookins, D.G., 1988. Eh–pH Diagrams for Geochemistry. Springer, New York. 176 pp.

Clayton, J.L., Rice, D.D., Michael, G.E., 1991. Oil-generating coals of the San Juan basin, New Mexico and Colorado, USA. Organic Chemistry 17, 735–742.

Close, J., 1997. Coalbed methane and coal geology. Earth-Science Reviews 42, 181–197.

Combaz, A., 1964. Les palynofacies. Revue de Micropaléontologie 7, 205–218.

Diessel, C.F.K., 1992. Coal-Bearing Depositional Systems. Springer, New York. 721 pp.

Dill, H.G., 1987. Environmental and diagenetic analyses of Lower Permian epiclastic and pyroclastic fan deposits—their role for coal formation and uranium metallogeny in the Stockheim Trough (F.R.G). Sedimentary Geology 52, 1–26.

Dill, H.G., 1989. Facies and provenance analysis of Upper Carboniferous to Lower Permian fan sequences at a convergent plate margin, using phyllosilicates, heavy minerals and rock fragments (Erbendorf Trough F.R. of Germany). Sedimentary Geology 69, 95–110.

Dill, H.G., 1995. Heavy mineral response to the progradation of an alluvial fan: implication concerning unroofing of source area, chemical weathering, and paleo-relief (Upper Cretaceous Parkstein fan complex/SE Germany). Sedimentary Geology 95, 39–56.

Dill, H.G., 1998. A review of heavy minerals in clastic sediments with case studies from the alluvial-fan through the nearshore-marine environments. Earth-Science Reviews 45, 103–132.

Dill, H.G., 2001. The geology of aluminum phosphates and sulfates of the alunite supergoup: a review. Earth-Science Reviews 53, 25–93.

Dill, H.G., Pöllmann, H., 2002. Chemical composition and mineral matter of paralic and limnic coal types of lignite through anthracite rank. Upper Carboniferous coal in comparison with Mesozoic and Cenozoic coals (Germany). Memoir-Canadian Society of Petroleum Geologists 19, 851–867.

Dill, H.G., Wehner, H., 1999. The depositional environment and mineralogical and chemical compositions of high ash brown coal resting on early Tertiary saprock (Schirnding Coal Basin, SE Germany). International Journal of Coal Geology 39, 301–328.

Dill, H.G., Teschner, M., Wehner, H., 1991. Geochemistry and lithofacies of Permo-Carboniferous carbonaceous rocks from the SW edge of the Bohemian Massif (Germany). A contribution to facies analysis of continental anoxic environments. International Journal of Coal Geology 18, 251–291.

Dill, H.G., Koch, J., Scheeder, G., Wehner, H., Strahl, J., 2002. Lithology, palynology and organic geochemistry of carbonaceous rocks in fluvial–lacustrine series of Tertiary to Quaternary age (Kathmandu Basin, Nepal). Neues Jahrbuch für Geologie und Paläontologie. Abhandlungen 227, 1–38.

Fan, W.M., Guo, F., Wang, Y.-J., Lin, G., 2003. Late Mesozoic calcalkaline volcanism of postorogenic extension in the northern Da Hinggan Mountains, northeastern China. Journal of Volcanology and Geothermal Research 121, 115–135.

Fielding, C.R., 1984. Upper delta plain, lacustrine and fluviolacustrine facies from the Westphalian of the Durham coalfield, NE England. Sedimentology 31, 547–567.

Fielding, C.R., 1986. Fluvial channel and overbank deposits from the Westphalian of the Durham coalfield, NE England. Sedimentology 33, 119–140.

Flores, R.M., 1981. Coal deposition in fluvial paleoenvironments of the Palaeocene Tongue River member of the Fort Union Formation, Powder River area, Powder River Basin, Wyoming and Montana. In: Ethridge, F.G., Flores, R.M. (Eds.), Recent and Ancient Non-Marine Depositional Environments: Models for Explorations, Spec. Publ.-Soc. Econ. Paleontol. Miner. 31, pp. 169–190.

Flores, R.M., 1983. Basin facies analysis of coal-rich Tertiary fluvial deposits, northern Powder River Basin, Montana and Wyoming. In: Collinson, J.D., Lewis, J. (Eds.), Modern and Ancient Fluvial Systems, Spec. Publ.-Intern. Assoc. of Sedim., vol. 6. Blackwell, Oxford, pp. 501–515.

Füchtbauer, H., Müller, G., 1970. Sediment-Petrologie, Part III. Schweizerbart, Stuttgart. 726 pp.

Galloway, W.E., Hobday, D.K., 1996. Terrigenous Clastic Depositional Systems—Applications to Fossil Fuel and Groundwater Resources. Springer, Heidelberg. 484 pp.

Gentzis, T., Goodarzi, F., Broussoulis, Y., 1990. Petrographic characteristics and depositional environment of Greek lignites: II. Ioannina Basin, Western Greece. Journal of Coal Quality 9, 53–61.

Gerel, O., 1998. Phanerozoic felsic magmatism and related mineralization in Mongolia. Bulletin of the Geological Society of Japan 49, 239–248.

Gomez, B., Martin-Closas, C., Meon, H., Thevenard, F., Barale, G., 2001. Plant taphonomy and palaeoecology in the lacustrine Una Delta. Palaeogeography, Palaeoclimatology, Palaeoecology 170, 133–148.

Halim, N., Kravchinsky, V., Gilder, S., Cogne, J.-P., Alexyutin, M., Sorokin, A., Courtillot, V., Chen, Y., 1998. A palaeomagnetic study from the Mongol–Okhotsk region: rotated Early Cretaceous volcanics and remagnetized Mesozoic sediments. Earth and Planetary Science Letters 159, 133–145.

Herngreen, G.F.W., Chlonova, A.F., 1981. Cretaceous microfloral provinces. Pollen et Spores 23, 441–555.

Herrmann, W., Blake, M., Doyle, M., Huston, D., Kamprad, J., Merry, N., Pontual, S., 2001. Short wavelenght infrared (SWIR) spectral analysis of hydrothermal alteration zones associated with base metal sulfide deposits at Rosebery and Western Tharsis, Tasmania, and Highway-Reward, Queensland. Economic Geology 96, 939–955.

Heunisch, C., 1990. Palynologie der Bohrung "Natzungen 1979", Blatt 4321 Borgholz (Trias, Oberer Muschelkalk 2,3, Unterer Keuper). Neues Jahrbuch für Geologie und Paläontologie. Monatshefte, 17–42.

Inci, U., 2002. Depositional evolution of Miocene coal successions in the Soma coalfield, western Turkey. International Journal of Coal Geology 51, 1–19.

Ishigaki, A., Ito, M., 2000. Size population of hummocky bedforms: an example from then Lower Cretaceous Chosi Group, northeastern Boso Peninsula, Japan. Journal of the Geological Society of Japan 106, 472–491.

Ito, M., Ishigaki, A., Nishikawa, T., Saito, T., 2001. Temporal variation in the wavelength of hummocky cross-stratification; implications for storm intensity through Mesozoic and Cenozoic. Geology 29, 87–89.

Jakobsen, B.H., 1988. Accumulation of pyrite and Fe-rich carbonate and phosphate minerals in a lowland moor area. Journal of Soil Science 39, 447–455.

Jargalsaikan, D., 1998. Mongolia—Mineral Resources and Mining Opportunities. Watkiss Studios, Biggleswade. 128 pp.

Jerram, D.A., 2001. Visual comparators for degree of grain-size sorting in two and three dimensions. Computers & Geosciences 27, 485–492.

Johnson, H.D., Levell, B.K., 1995. Sedimentology of a transgressive, estuarine sand complex: the Lower Cretaceous Woburn Sands (Lower Greensand), southern England. International Association of Sedimentologists 22, 17–46.

Kampe, A., 1994. Kohlen der Mongolei. BGR report (unpublished), Hannover. 55 pp.

Kemper, E., Zimmerle, W., 1982. Die Tuffe des Apt- und Alb-Nordwestdeutschlands. Geologisches Jahrbuch, A 65, 245–257.

Khand, Yo., Badagarav, D., Ariunchimeg, Ya., Barsbold, R., 2000. Cretaceous System in Mongolia and its Depositional Environment. In: Okada, H., Mateer, N.J. (Eds.), Cretaceous Environments of Asia. Elsevier, Amsterdam, pp. 49–79.

Lensing, H., Vogt, M., Herrling, B., 1995. Modellierung der Redoxsequenz in einer Uferfiltrationspassage unter direkter Berücksichtigung der prozeßsteuernden Bakteriengruppen. In: Schöttler, U. (Ed.), Schadstoffe im Grundwasser. Deutsche Forschungsgemeinschaft, Weinheim, pp. 439–474.

Lundegard, P.D., Samuels, N.D., 1980. Field classification of fine-grained rocks. Journal of Sedimentary Petrology 50, 781–786.

Makaske, B., 2001. Anastomosing rivers: a review of their classification, origin and sedimentary products. Earth-Science Reviews 53, 149–196.

Malumian, N., Carames, A., 1997. Upper Campanian–Paleogene from the Rio Turbio coal measures in southern Argentina; micropaleontology and the Paleocene/Eocene boundary. Journal of South American Earth Sciences 10, 189–201.

Marinov, N.A., 1973. Geology of the People's Republic of Mongolia: Stratigraphy. Nedra, Moskau. 583 pp. (in Russian).

Marinov, N.A., Hasin, R.A., Hurts, A., 1973. Geology of the People's Republic of Mongolia: Magmatism and Tectonic. Nedra, Moskau. 751 pp. (in Russian).

Markic, M., Sachsenhofer, R.F., 1997. Petrographic composition and depositional environments of the Pliocene Velenje lignite seam (Slovenia). International Journal of Coal Geology 33, 229–254.

McCabe, P.J., 1984. Depositional environments of coal and coal-bearing strata. In: Rahmani, R.A., Flores, R.M. (Eds.), Sedimentology of Coal and Coal-bearing Sequences, Spec. Publ. Inter. Assoc. Sedimentologists, vol. 7, pp. 13–42.

McCabe, P.J., Parrish, J.T., 1992. Controls on the Distribution and Quality of Cretaceous Coals. Geolocical Society of America. Special Paper 267, 400 pp.

Miall, A.D., 1996. The Geology of Fluvial Deposits. Springer, Berlin. 582 pp.

Miall, A.D., 2000. Principles of Sedimentary Basin Analysis. 3rd ed. Springer, Berlin. 616 pp.

Morse, J.W., Berner, R.A., 1995. What determines sedimentary C/S ratios. Geochimica et Cosmochimica Acta 59, 1073–1077.

Okada, H., Mateer, N.J., 2000. Cretaceous Environments of Asia. Elsevier, Amsterdam. 255 pp.

Pelzer, G., Riegel, W., Wilde, V., 1992. Depositional control on the lower cretaceous wealden coals of Northwest Germany. Special Paper-Geological Society of America 267, 227–244.

Pettijohn, F.J., Potter, P.E., Siever, R., 1987. Sand and Sandstone. Springer, New York. 618 pp.

Rao, P.D., Walsh, D.E., 1999. Influence of environments of coal deposition on phosphorous accumulation in a high latitude, northern Alaska, coal seam. International Journal of Coal Geology 33, 19–42.

Reineck, H.-E., Singh, I.B., 1980. Depositional Sedimentary Environments. With Reference to Terrigenous Clastics. Springer, New York. 549 pp.

Reinink-Smith, L.M., 1990. Mineral assemblages of volcanic and detrital partings in tertiary coal beds, Kenai Peninsula, Alaska. Clays and Clay Minerals 38, 97–108.

Schaefer, R.G., Püttmann, W., 1987. Analysis of hydrocarbons in coals by means of microthermodesorption-capillary gas chromatography combination. Journal of Chromatography 395, 203–216.

Schäfer, A., Hilger, D., Gross, G., von der Hocht, F., 1995. Cyclic sedimentation in Tertiary Lower-Rhine Basin (Germany)—the "Liegendrücken" of the brown-coal open-cast Fortuna mine. Sedimentary Geology 103, 229–247.

Scott, A.C., 2000. The Pre-Quaternary history of fire. Palaeogeography, Palaeoclimatology, Palaeoecology 164, 357–380.

Scott, A.C., Jones, T.P., 1994. The nature and influence of fire in Carboniferous ecosystems. Palaeogeography, Palaeoclimatology, Palaeoecology 106, 91–112.

Sha, J., Cai, H., He, C., Gu, Z., Jiang, J., Yin, D., Zhao, X., Liu, Z., Jiang, B., 2002. Studies on the Early Cretaceous Longzhaogou and Jixi Groups of eastern Heilongjing, northeast China, and their bearing on the age of supposedly Jurassic strata in eastern Asia. Journal of Asian Earth Sciences 20, 141–150.

Stach, E., Mackowsky, M.Th., Teichmüller, M., Taylor, G.H., Chandra, D., Teichmüller, R., 1982. Stach's Textbook of Coal Petrology. Gebr. Borntraeger, Berlin. 535 pp.

Thomas, L., 2002. Coal Geology. John Wiley & Sons, New York. 384 pp.

Traynor, J.J., Sladen, C., 1995. Tectonic and stratigraphy evolution of the Mongolian People's Republic and its influence on hydrocarbon geology and potential. Marine and Petroleum Geology 12, 35–52.

Tripathi, A., 2001. Permian, Jurassic and Early Cretaceous palynofloral assemblages from subsurface sedimentary rocks in Chuperbhita Coalfield, Rajmahal Basin, India. Review of Palaeobotany and Palynology 113, 237–259.

Tucker, M., 2001. Sedimentary Petrology. Blackwell, London. 262 pp.

Tuttle, M.L., Goldhaber, M.B., 1993. Sedimentary sulfur geochemistry of the Paleogene Green River Formation, Western USA: implications for interpreting depositional and diagenetic processes in saline alkaline lakes. Geochimica et Cosmochimica Acta 57, 3023–3039.

Van Bergen, P.F., Kerp, J.H.F., 1990. Palynofacies and sedimentary environments of a Triassic section in southern Germany. Mededelingen-Rijks Geologische Dienst 45, 23–38.

Virtanen, K., 1994. Geological control of iron and phosphorous precipitates in mires of the Ruukki–Vihanti area, central Finland. Bulletin-Geological Survey of Finland 375, 1–69.

Visscher, H., Brugman, W.A., 1981. Ranges of selected palynomorphs in the Alpine Triassic of Europe. Review of Palaeobotany and Palynology 34, 115–128.

Ward, C.R, 1978. Mineral matter in Australian bituminous coal. Proceedings of the Australian Institute of Mineralogy and Metallurgy 267, 7–25.

Yagishita, K., Arakawa, S., Taira, A., 1992. Grain fabrics of hummocky and swaley cross-stratification. Sedimentary Geology 78, 181–189.

Yi, S., Batten, D.J., Yun, H., Park, S.-J., 2002. Cretaceous and Cenozoic non-marine deposits of the Northern South Yellow Sea Basin, offshore western Korea: palynostratigraphy and palaeoenvironments. Palaeogeography, Palaeoclimatology, Palaeoecology 191, 15–44.

Zeman, J., 1989. Supergene alteration of sulfides: III. Corrosion of sulfides in galvanic contact. Scripta 19, 113–124.

Zhi-chen, Song, Liu, Gen-wu, Li, Wen-ben, Jia, Bin-li, Hua, Ru-Hong, 1987. Early Cretaceous palynological assemblages from Eren Basin, NE Mongolia. Cenozoic–Mesozoic Palaeontology and Stratigraphy of East China, Peking. 335 pp.